1-1-2011

The Australian methane budget: interpreting surface and train-borne measurements using a chemistry transport model

A Fraser
University of Edinburgh

C C. Miller
Harvard University

Paul Palmer
University of Edinburgh, pip@ed.ac.uk

Nicholas M. Deutscher
University of Wollongong, ndeutsch@uow.edu.au

Nicholas B. Jones
University of Wollongong, njones@uow.edu.au

See next page for additional authors

The Australian methane budget: interpreting surface and train-borne measurements using a chemistry transport model

Abstract

We investigate the Australian methane budget from 2005-2008 using the GEOS-Chem 3D chemistry transport model, focusing on the relative contribution of emissions from different sectors and the influence of long-range transport. To evaluate the model, we use in situ surface measurements of methane, methane dry air column average (XCH 4) from ground-based Fourier transform spectrometers (FTSs), and train-borne surface concentration measurements from an in situ FTS along the north-south continental transect. We use gravity anomaly data from Gravity Recovery and Climate Experiment to describe the spatial and temporal distribution of wetland emissions and scale it to a prior emission estimate, which better describes observed atmospheric methane variability at tropical latitudes. The clean air sites of Cape Ferguson and Cape Grim are the least affected by local emissions, while Wollongong, located in the populated southeast with regional coal mining, samples the most locally polluted air masses (2.5% of the total air mass versus <1% at other sites). Averaged annually, the largest single source above background of methane at Darwin is long-range transport, mainly from Southeast Asia, accounting for ~25% of the change in surface concentration above background. At Cape Ferguson and Cape Grim, emissions from ruminant animals are the largest source of methane above background, at approximately 20% and 30%, respectively, of the surface concentration. At Wollongong, emissions from coal mining are the largest source above background representing 60% of the surface concentration. The train data provide an effective way of observing transitions between urban, desert, and tropical landscapes. Copyright Copyright 2011 by the American Geophysical Union.

Keywords

Australian, methane, budget, interpreting, surface, train, borne, measurements, using, chemistry, transport, model, GeoQUEST

Disciplines

Life Sciences | Physical Sciences and Mathematics | Social and Behavioral Sciences

Publication Details

Fraser, A., Miller, C. Chan., Palmer, P. I., Deutscher, N. M., Jones, N. B. & Griffith, D. W. T. (2011). The Australian methane budget: interpreting surface and train-borne measurements using a chemistry transport model. Journal of Geophysical Research D: Atmospheres, 116 (20), 1-22.

Authors

A Fraser, C C. Miller, Paul Palmer, Nicholas M. Deutscher, Nicholas B. Jones, and David W. Griffith

The Australian methane budget: Interpreting surface and train-borne measurements using a chemistry transport model

Annemarie Fraser,[1] Christopher Chan Miller,[2,3] Paul I. Palmer,[1] Nicholas M. Deutscher,[2,4] Nicholas B. Jones,[2] and David W. T. Griffith[2]

Received 18 March 2011; revised 4 August 2011; accepted 4 August 2011; published 22 October 2011.

[1] We investigate the Australian methane budget from 2005–2008 using the GEOS-Chem 3D chemistry transport model, focusing on the relative contribution of emissions from different sectors and the influence of long-range transport. To evaluate the model, we use in situ surface measurements of methane, methane dry air column average (XCH_4) from ground-based Fourier transform spectrometers (FTSs), and train-borne surface concentration measurements from an in situ FTS along the north–south continental transect. We use gravity anomaly data from Gravity Recovery and Climate Experiment to describe the spatial and temporal distribution of wetland emissions and scale it to a prior emission estimate, which better describes observed atmospheric methane variability at tropical latitudes. The clean air sites of Cape Ferguson and Cape Grim are the least affected by local emissions, while Wollongong, located in the populated southeast with regional coal mining, samples the most locally polluted air masses (2.5% of the total air mass versus <1% at other sites). Averaged annually, the largest single source above background of methane at Darwin is long-range transport, mainly from Southeast Asia, accounting for ~25% of the change in surface concentration above background. At Cape Ferguson and Cape Grim, emissions from ruminant animals are the largest source of methane above background, at approximately 20% and 30%, respectively, of the surface concentration. At Wollongong, emissions from coal mining are the largest source above background representing 60% of the surface concentration. The train data provide an effective way of observing transitions between urban, desert, and tropical landscapes.

Citation: Fraser, A., C. Chan Miller, P. I. Palmer, N. M. Deutscher, N. B. Jones, and D. W. T. Griffith (2011), The Australian methane budget: Interpreting surface and train-borne measurements using a chemistry transport model, *J. Geophys. Res.*, *116*, D20306, doi:10.1029/2011JD015964.

1. Introduction

[2] Over a 20-year time frame, methane (CH_4) has a radiative forcing comparable to carbon dioxide, reflecting its direct and indirect impacts on Earth's radiation balance [*Intergovernmental Panel on Climate Change* (*IPCC*), 2007]. The global budget of atmospheric methane is well quantified via sparse but highly accurate surface concentration measurements, but there is much more uncertainty in attributing observed large-scale concentration changes to emissions from individual geographical regions and from individual sectors [e.g., *Rigby et al.*, 2008; *Dlugokencky et al.*, 2009; *Bloom et al.*, 2010]. The global total methane budget is approximately evenly split between anthropogenic and natural sources. In this paper we investigate the relative contribution of local emissions and long-range transport in the Australian methane budget from 2005 to 2008 using the GEOS-Chem 3D chemistry transport model. To evaluate the model, we use measurements from Darwin (12.4°S, 130.9°E), Cape Ferguson (19.3°S, 147.1°E), Wollongong (34.4°S, 150.9°E), and Cape Grim (40.7°S, 144.7°E) and measurements taken from the Ghan train that covers a north–south continental transect.

[3] The atmospheric concentration of methane is determined by anthropogenic and natural sources and from the atmospheric loss due to oxidation by the hydroxyl radical (OH), the exchange between the troposphere and stratosphere, and a soil sink. The resulting lifetime is 8.7 ± 1.3 years [*IPCC*, 2007]. Anthropogenic sources include

[1]School of GeoSciences, University of Edinburgh, Edinburgh, UK.
[2]School of Chemistry, University of Wollongong, Wollongong, New South Wales, Australia.
[3]Now at Department of Earth and Planetary Sciences, Harvard University, Cambridge, Massachusetts, USA.
[4]Now at Institute of Environmental Physics, University of Bremen, Bremen, Germany.

0148-0227/11/2011JD015964

ruminant animals, rice cultivation, fossil fuel production, landfills, and biomass burning [e.g., *Olivier et al.*, 2005]. Natural sources include wetlands, termites, oceans, and methane hydrates [e.g., *Fung et al.*, 1991]. The largest single source is from wetlands, which account for one third of all global emissions of methane to the atmosphere [e.g., *Bloom et al.*, 2010]. Further details about the individual sources and sinks are in section 5.

[4] The Australian methane budget includes contributions from all globally important sources of methane, with the exception of methane hydrates, reflecting its heterogeneous landscape [*Wang and Bentley*, 2002]. Anthropogenic emission estimates are better characterized than natural sources mainly due to the geographical extent and spatial and temporal variations associated with the natural sources, presenting a considerable weakness of current emission inventories. Past studies of wetland distribution in Australia have focused on subtropical arid regions [e.g., *Boon et al.*, 1997; *Roshier et al.*, 2001; *Roshier and Rumbachs*, 2004], but recent work has shown that wetlands in the tropics also contribute significantly to the total methane budget of Australia [*Deutscher et al.*, 2010a]. Over the northernmost regions of the country, there is also import of air from the chemical northern hemisphere when the chemical equator, partly determined by the position of the intertropical convergence zone, lies to the south of the geographical equator [*Hamilton et al.*, 2008]. Figure 1 shows the methane measurement network over Australia that we use for our study. Until 2005, the only long-term measurements of methane in Australia were in situ surface measurements made at Cape Grim and Cape Ferguson. Since then, the data coverage has increased with the installation of ground-based Fourier transform spectrometers (FTSs) with shortwave infrared (SWIR) measuring capability at Darwin (in 2005) and Wollongong (in 1996, SWIR measurements began in 2008) as part of the Total Carbon Column Observing Network (TCCON) [*Wunch et al.*, 2011; *Deutscher et al.*, 2010b]. In addition, five measurement campaigns have been held with an in situ FTS installed on the Ghan train, which runs between Adelaide (34.9°S, 138.6°E) and Darwin [*Deutscher et al.*, 2010a]. A similar in situ FTS has provided data at Darwin since 2007.

[5] In section 2 we present anthropogenic and natural sources of methane in Australia. Section 3 discusses the meteorology of surface winds at the four measurement sites. Sections 4 and 5 describe the measurements and the GEOS-Chem model used in this study, respectively. In section 6, we construct an inventory of emissions from wetlands in northern tropical Australia based on space-based gravity anomaly measurements. In section 7 we compare the model and measurements from 2005–2008, including a discussion about the individual geographical regions and sectors that contribute to the model over the measurement sites. Finally, we conclude the paper in section 8.

2. Australian Methane Inventory

[6] The Government of Australia produces an annual estimate of anthropogenic greenhouse gas emissions (National Greenhouse Gas Inventory, NGGI), including energy (which includes mining-related emissions), industrial processes, enteric fermentation from ruminant animals, manure management, rice cultivation, prescribed burning of savannas, field burning of agricultural residues, and landfills and wastewater handling. For 2008, the NGGI reports the release of 5.6 Tg of CH_4, or 120 Tg equivalent CO_2, equating to 20% of Australia's total anthropogenic greenhouse gas emissions [*Department of Climate Change*, 2010]. Table 1 lists the sources considered in the inventory for 2008. The reported uncertainty on the total inventory (including carbon dioxide and other greenhouse gases) is only 2%, while reported uncertainties associated with individual source categories range from 5% to 50%. Enteric fermentation from ruminant animals is the largest source of methane in Australia, accounting for 58% of anthropogenic emissions. These emissions are located across the country, with the largest concentration in the more populated regions of New South Wales (NSW), Queensland (QLD), and Victoria (VIC). Energy production, mainly a result of coal mining in NSW and QLD, accounts for 30% of anthropogenic emissions. Landfills and wastewater handling are the next largest source at 12%, and are located near population centers. In the inventories used in this work (described in section 5), methane emissions from Australia are between 9 and 10 Tg/year, of which 5–6 Tg/year are attributed to anthropogenic sources and 4–5 Tg/year are attributed to natural sources.

[7] Methane is produced in wetlands by anaerobic decomposition of organic matter by methanogenic bacteria. The amount of methane produced is highly variable and is most related to temperature and the depth of the water table. Recent work has estimated that wetlands in northern Australia emit on the order of 1 Tg CH_4/year and account for 40%–65% of natural emissions, or 10%–20% of all emissions in Australia [*Deutscher et al.*, 2010a]. Earlier work found that permanent and seasonal wetlands in Australia emit similar amounts of methane [*Dalal et al.*, 2008] (where seasonal wetlands are referred to as ephemeral wetlands). Wetlands in southern Australia emit a further 1 Tg of methane [*Bloom et al.*, 2010]. Wetland inundation in Australia can vary significantly from year to year [e.g., *Boon et al.*, 1997], implying that changes in methane emissions from wetlands can have a significant impact on the year to year changes in the Australian methane budget. Wetlands will be further discussed in section 6.

[8] Emissions from coastal oceans are related to microbial activity and are poorly understood. Recent work suggests a link between methane production and the decomposition of phosphorous-containing organic compounds, with emissions related to available phosphorous and nitrates [*Karl et al.*, 2008]. Emissions from oceans surrounding Australia are on the order of 1 Tg CH_4 per year [*Houweling et al.*, 1999]. The global emissions were derived by uniformly distributing the global flux strength determined over the open ocean and continental shelves [*Lambert and Schmidt*, 1993; *Houweling et al.*, 1999].

[9] Termites produce methane by decomposing organic material via a symbiotic relationship with anaerobic bacteria. Emissions from termites are a significant source of methane in Australia, emitting approximately 1 Tg CH_4 per year [*Fung et al.*, 1991]. *Fung et al.* [1991] derived the global inventory of emissions using a global vegetation database and distributing an aseasonal source over the known habitats of termites. Termites are present throughout the country, with the largest emissions in the Northern Territory (NT), northwestern QLD, and northern Western Australia (WA) and

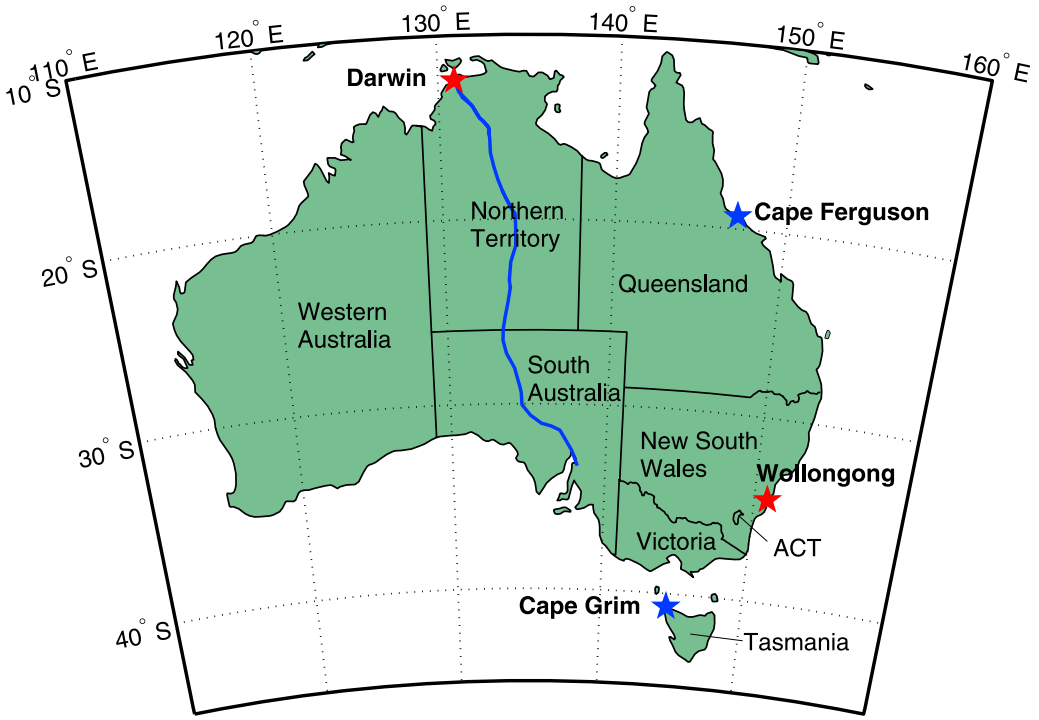

Figure 1. Location of methane measurement sites in Australia. Red stars indicate TCCON sites [*Wunch et al.*, 2011], blue stars are flask sampling sites [*Prinn et al.*, 2000; *Dlugokencky et al.*, 2009; *Francey et al.*, 1996]. The blue line shows the path of the Ghan train [*Deutscher et al.*, 2010a].

South Australia (SA). Emissions from termites vary between species, individual mounds within a species, temperature, and moisture [*Fraser et al.*, 1986]. Emissions from termites are not well characterized, due to uncertainties in individual termite mound production and location, and issues in scaling up from measurements of individual mounds to the regional and global scales.

3. Meteorology

[10] Figure 2 shows the seasonal distribution of surface winds over Australia, taken from the GEOS-5 analyzed meteorology and averaged on a 2° × 2.5° horizontal resolution for January 2004–December 2009 (see section 5). During the austral summer (December-January-February, DJF), Darwin is affected by the Australian-Indonesian monsoon, characterized by a reversal in the winds in the lower troposphere from dry easterlies to moist westerlies [*Wheeler and McBride*, 2005]. The monsoon brings warm, moist air from the Southeast Asian tropics. As a result, at Darwin in the wet season (DJF, see Figure 2a) surface winds are primarily from the west and north. As the monsoon weakens in March-April-May (MAM, Figure 2b), surface winds are progressively from the south and east, bringing dry continental air northward. This pattern persists through June-July-August (JJA, Figure 2c). In September-October-November (SON, Figure 2d), as monsoon weather begins again, surface winds are from the north and east, becoming more easterly as the season progresses.

[11] At Cape Ferguson the winds are from the east throughout the wet season (DJF), bringing clean Pacific air to the site. There is a gradual shift of the surface winds so that by MAM the winds are from the southeast. This circulation continues through JJA, eventually shifting back to easterlies during SON.

Table 1. Methane Emissions for 2008 Broken Down by Source Category and States and Territories[a]

Category	ACT	NSW	NT	QLD	SA	TAS	VIC	WA
Energy	1.0	925.6	4.6	473.2	54.9	8.9	87.8	87.9
Industrial processes	0.0	2.4	0.0	0.0	0.5	0.0	0.0	0.0
Enteric fermentation	1.0	585.5	120.2	985.9	158.7	68.8	463.3	262.0
Manure management	0.0	19.5	0.1	23.1	10.8	2.4	23.8	6.2
Rice cultivation	0.0	2.0	0.0	0.0	0.0	0.0	1.3	0.0
Prescribed burning of savannas	0.0	1.0	234.2	48.4	0.8	0.1	1.3	169.0
Field burning of agricultural residues	0.0	2.4	0.0	2.0	1.1	0.0	0.9	2.7
Landfills and wastewater handling	4.5	245.1	5.3	143.7	37.2	13.0	158.0	57.0

[a]Methane emissions are measured in Gg [*Department of Climate Change*, 2010]. ACT is the Australian Capital Territory, NSW is New South Wales, NT is the Northern Territory, QLD is Queensland, SA is South Australia, TAS is Tasmania, VIC is Victoria, and WA is Western Australia. See Figure 1 for the location of the states and territories.

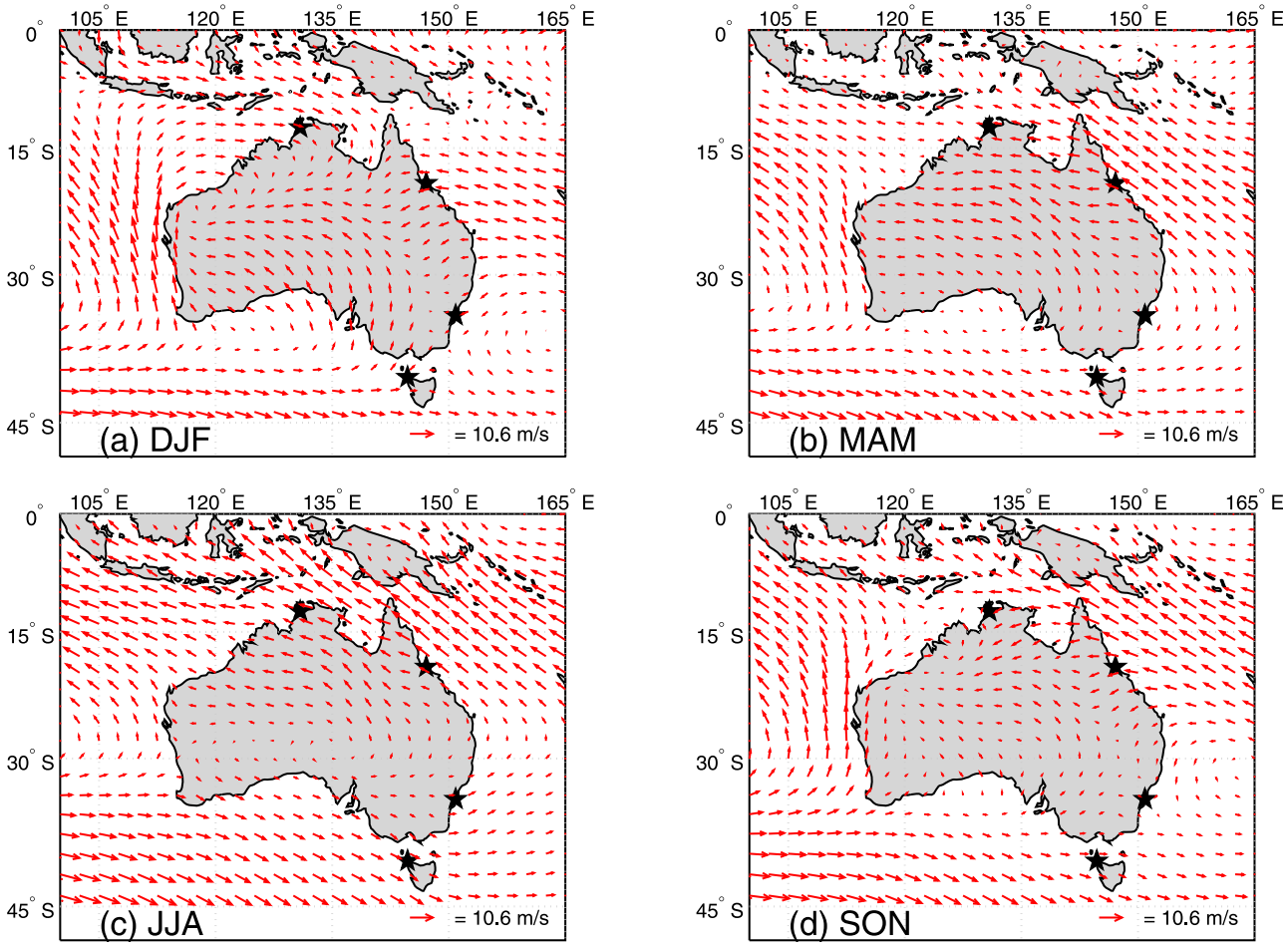

Figure 2. Seasonal winds for Australia from GEOS-5 at 2° × 2.5° resolution from January 2004 to December 2009. The black stars denote the locations of the four measurements sites, from north to south: Darwin, Cape Ferguson, Wollongong, and Cape Grim.

[12] At Wollongong the climatologically averaged winds are weak (<4m/s) throughout the year. Surface winds are strongest during the winter (JJA), bringing continental air from the west over Wollongong. These winds weaken through the spring (SON), are fairly quiescent in the summer (DJF), and begin to strengthen again in the autumn (MAM). In the summer there are local E-NE sea breezes which affect local in situ concentrations.

[13] Throughout the year, winds at Cape Grim bring clean air from the Indian Ocean over the measurement site. The winds are strongest in the winter (JJA), when they are from the northwest. The winds weaken over the spring (SON) and shift to a more westerly flow. During summer months (DJF) winds are at their weakest and from the southwest. During the autumn months (MAM) surface winds begin to strengthen again and shift back to a westerly flow.

4. Measurements

[14] Figure 1 shows the location of the TCCON instruments, the flask sampling sites, and the path of the Ghan train used in this work to evaluate the GEOS-Chem model. TCCON is a global network of ground-based solar Fourier transform spectrometers operating in the shortwave infrared (http://www.tccon.caltech.edu/), which was developed to provide a continuous, long-term data set for satellite validation and carbon budget studies [e.g., *Wunch et al.*, 2011]. Here, we use methane data from two Australian sites: Darwin, NT (12.5°S, 130.9°E) [*Deutscher et al.*, 2010b] and Wollongong, NSW (34.4°S, 150.9°E).

[15] Column-average dry-air mole fractions of CH_4 (XCH_4) at the TCCON sites are derived from high-resolution solar absorption spectra, acquired using a Bruker IFS125/HR FTS spectrometer over a bandwidth of 3800–15,800 cm^{-1} and with a spectral resolution of 0.02 cm^{-1} [*Wunch et al.*, 2011]. Column abundances are retrieved from the spectra using the nonlinear least squares fitting algorithm GFIT, developed at NASA-JPL. GFIT iteratively minimizes the RMS difference between the measured and calculated spectra by scaling the a priori gas profiles. The average of three microwindows centered at 5938, 6002, and 6076 cm^{-1} is used for CH_4. O_2 is retrieved in a microwindow covering the 7882 cm^{-1} band. XCH_4 is calculated relative to the O_2 column (molecules/cm^2):

$$X_{CH4} = 0.2095 \frac{columnCH_4}{columnO_2}, \quad (1)$$

Table 2. Annual Global and Australian Emission Estimates of Methane Broken Down by Sector[a]

Source	Global	Australia
Anthropogenic Sources		
Ruminant animals	88.7–92.5	2.65–2.86
Coal mining	40.5–47.0	0.74–0.80
Oil production	34.8–42.7	0.64–0.75
Landfills	44.6–44.7	0.62–0.66
Biomass burning	14.8–15.4	0.31–0.67
Biofuel burning	1.14	0.003
Rice cultivation	60.8–60.9	0.00
Total anthropogenic	285.3–304.3	4.96–5.74
Natural Sources		
Wetlands	189.0–197.5	0.26–0.61
Permanent wetlands	0.0	0.47
Seasonal wetlands	0.0	0.16–0.65
Termites	20.0	1.40
Oceans	15.0	1.51
Methane hydrates	5.0	0.00
Total natural	229.0–237.5	3.80–4.64
Total	514.3–541.8	8.76–10.38

[a]Emission estimates measured in Tg/year. The range of values given represents the range of the annual values for 2005–2008.

which reduces the effect of measurement and instrumental errors that are common to both gases and improves the precision of the column measurement. The precision of the methane measurements is 0.2% (3.5 ppb of a column of 1750 ppb), though the accuracy is limited by spectroscopic parameters. Recent comparisons suggest that a correction of 2.2% (38.5 ppb) is needed to bring the TCCON measurements in line with colocated aircraft profiles, the uncertainty on this correction leads to a cited accuracy of 7 ppb [*Wunch et al.*, 2010]. This correction additionally brings the TCCON column measurements onto the same scale as the surface in situ measurements, allowing them to be used in modeling studies.

[16] The train-borne and Darwin in situ FTS measurements are acquired using a 20 m (26 m for the Darwin instrument) path length multipass White cell coupled to a 1 cm^{-1} Bruker IRcube. A continuously flowing air sample is dried and drawn through the White cell and spectra coadded for 5 min (10 min for Darwin). The resulting spectra are analyzed using the Multiple Atmospheric Layer Transmission (MALT) nonlinear least squares fitting software [*Griffith*, 1996, 2002; *Griffith et al.*, 2011]. MALT generates a modeled spectrum from initial estimates of gas concentrations and instrument line shape and the best-fit calculation provides concentrations of the species present in the spectrum. Methane is retrieved from a window covering 3001–3150 cm^{-1}. The precision, calculated by the standard deviation of repeated measurements, is 0.2 ppb.

[17] Three ground-based flask networks make regular measurements of surface methane over Australia using gas chromatography: the NASA Advanced Global Atmospheric Gases Experiment (AGAGE), released November 2009 [*Prinn et al.*, 2000; *Cunnold et al.*, 2002]; the NOAA Earth System Research Laboratory (ESRL), version 2009-06-18 [*Dlugokencky et al.*, 2009]; and the CSIRO Global Atmospheric Sampling Laboratory (GASLab), released August 2009 [*Francey et al.*, 1996]. The AGAGE network takes hourly measurements, while the others collect weekly flask samples. Cape Ferguson is part of the GASLab network, and data are available from 1991. Cape Grim is part of all three networks: GASLab and ESRL measurements are available from 1984, while AGAGE measurements are available from 1993. The GASLab and ESRL measurements have a precision of 1.5 ppb [*Dlugokencky et al.*, 2009]. The AGAGE measurements at Cape Grim have a precision of 1.7 ppb [*Cunnold et al.*, 2002].

5. The GEOS-Chem Chemistry Transport Model

[18] GEOS-Chem is a 3-D global chemical transport model (version v8-01-01) driven by version five of the assimilated meteorological fields from the NASA Global Modeling and Assimilation Office. We use the model with a horizontal resolution of 2° × 2.5° with 47 vertical levels. Anthropogenic emissions from ruminant animals, coal mining, oil production, and landfills are from the Emission Database for Global Atmospheric Research, Fast Track (EDGAR 3.2 FT) inventory [*Olivier et al.*, 2005]. To account for interannual variability, we adjust these emissions by country-specific socioeconomic factors [*Wang et al.*, 2004]. For Australia, the emissions are adjusted to the NGGI estimates [*Department of Climate Change*, 2010].

[19] The model uses biomass burning estimates from the Global Fire Emissions Database (GFED v2) inventory, which include both seasonal and interannual variation [*van der Werf et al.*, 2006]. Biofuel burning emissions are from *Yevich and Logan* [2003]. Natural sources from oceans [*Houweling et al.*, 1999], termites, and hydrates are included, as well as a soil sink [*Fung et al.*, 1991]. We assume these emissions are constant throughout the study period. Emissions from rice and wetlands vary seasonally and from year to year, based on a top-down study [*Bloom et al.*, 2010].

[20] The tropospheric OH sink is described by monthly mean 3-D OH fields generated from a full-chemistry O_x-NO_x-VOC run of the GEOS-Chem model [*Fiore et al.*, 2003]. Using these OH fields, we have modeled concentrations of methyl chloroform (CH_3CCl_3, MCF). OH is the major destruction pathway for MCF, and measurements of MCF are a common method of determining the global OH field. We find a lifetime of MCF of 4.8 ± 0.1 years in the model, which is consistent with the 4.9 ± 0.3 years found by *Prinn et al.* [2005]. Loss rates for methane in the stratosphere are adapted from a 2-D stratospheric model [*Wang et al.*, 2004]. Fixing the OH sink allows a linear decomposition of methane contribution from regional sources.

[21] Table 2 reports the global and Australian methane budget estimates used in the model, broken down by sector for 2005–2008. Figure 3 shows the regions in and adjacent to Australia used in the tracer runs. We divide Australia into four regions: the West Tropical region (WTA) consisting of northern areas of Western Australia and the Northern Territory, the East Tropical region (ETA) consisting of Tropical Queensland, Metropolitan Australia consisting of the more populated south and eastern coasts, and the Desert region, which consists of the rest of Australia. Tracers for North and South America, Europe, Africa, Eurasia, Southeast Asia (SE Asia), the Southern Hemisphere Tropics (consisting of the Asian islands south of the equator), New Zealand (NZ), and the rest of the world (ROW) are also included. For each of the four Australian regions there are tracers for each relevant methane source (ten each for the tropical regions, nine each for the other two regions).

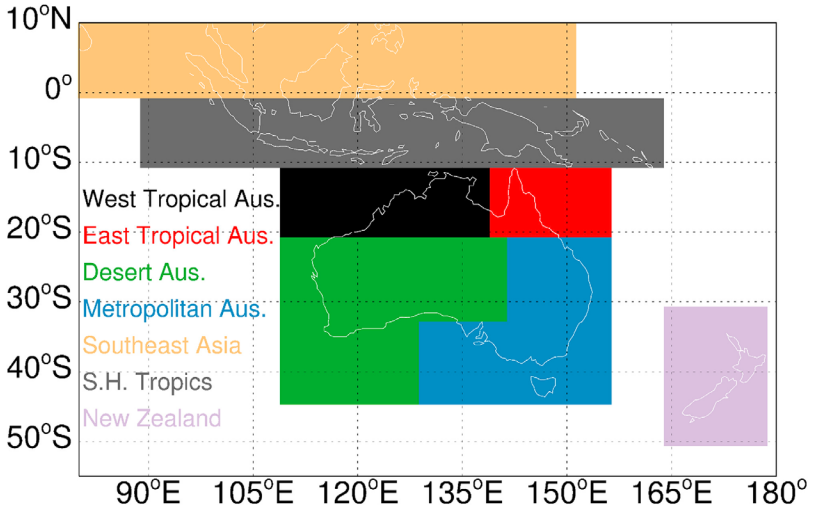

Figure 3. Tagged regions used in the GEOS-Chem simulations. The regions not shown are as follows: North America (24°N–88°N, 172.5°W–17.5°W), South America (56°S–24°N, 112.5°W–32.5°W), Africa (48°S–36°N, 17.5°W–60°E), Europe (36°N–88°N, 17.5°W–45°E), Eurasia (45°N–88°N, 45°E–180°E and 36°N–45°N, 45°E–60°E), and Southeast Asia (0°–45°N, 60°E–150°E). The rest of the world, consisting mainly of the oceans, South Pacific Islands, and Antarctica is also carried forward as a tracer.

In the other regions only the total source is carried forward, giving a total of 48 tracers (47 tracers plus the total global methane).

[22] To minimize the effects of the initial conditions and avoid the need to run the model with all 48 tracers for decades, we have chosen to set the tracers to zero at the beginning of every month, which allows us to study the influence of transport and emissions from month to month. While this also resets the influence of long-range transport, the monthly variations in transport and emissions

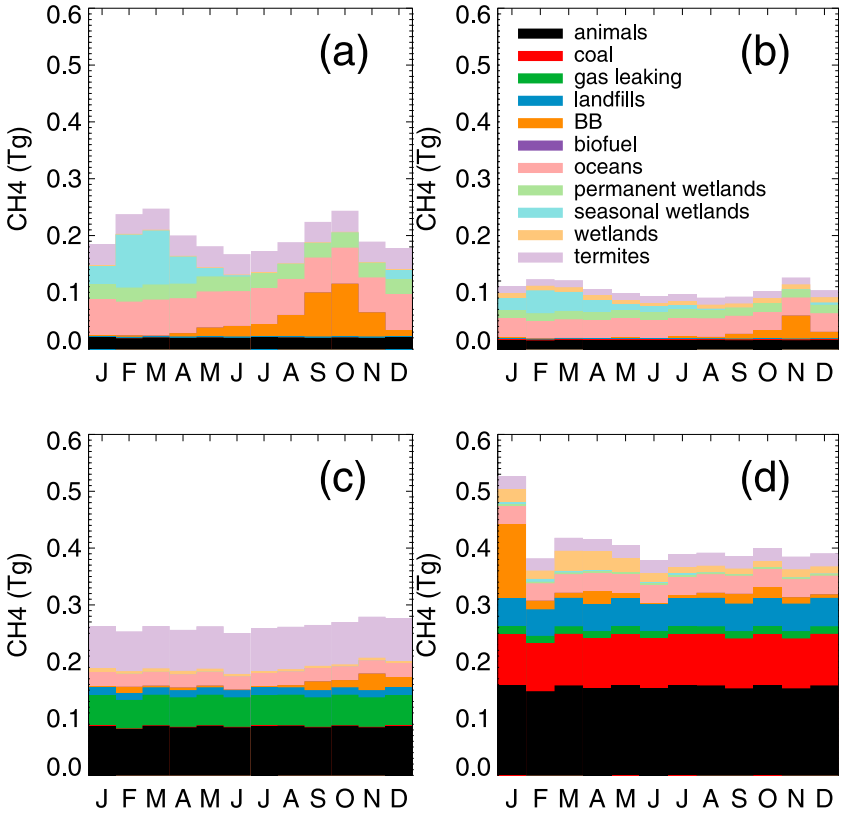

Figure 4. Monthly mean methane emissions from tagged sources for 2008 for the four Australian regions: (a) West Tropical Australia, (b) East Tropical Australia, (c) Desert Australia, and (d) Metropolitan Australia.

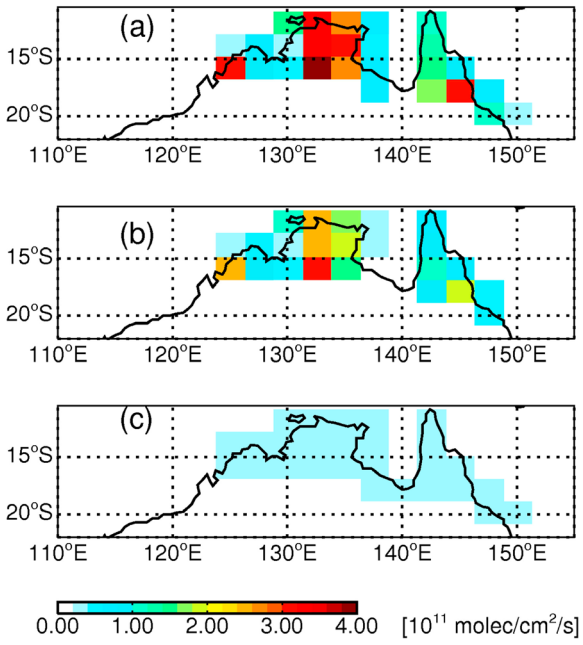

Figure 5. Tropical Australia seasonal wetlands emissions (NEWWET) derived from GRACE gravity anomaly data, averaged on the GEOS-Chem 2° × 2.5° grid, and scaled to the estimates of *Deutscher et al.* [2010a] for (a) 23 February to March 2 2008 and (b) 24 March to 2 April 2008, and (c) permanent wetlands emissions.

are more clearly represented. As a result, the individual tagged tracers represent only a small fraction of the total column of methane. We refer to this fraction as the signal above background, or the additional source of methane. The background we define as the difference between the total tracer and the sum of the monthly, geographically disaggregated tagged tracers.

[23] The initial total global methane in 2005 was produced by running the model for 6 years beginning with an initial field in January 1999 which was constructed from the surface flask measurements for that month. Six broad geographical regions were defined by latitude. In each region the mean of the flask measurements was used to initialize the surface concentration.

[24] Figure 4 shows the monthly emissions (Tg) in the four different Australian regions. Wetlands refers to the wetlands in the south of Australia. Permanent and seasonal wetlands refer to wetlands in the north of Australia that will be discussed in section 6. In West Tropical Australia emissions are dominated by oceans, seasonal wetlands in the wet season and soon after (DJF-MAM), and biomass burning in the dry season (SON). Termites and permanent wetlands are also significant sources. In East Tropical Australia oceans are the largest source, with significant contributions from seasonal wetlands in the wet season and soon after and biomass burning in the dry season. In the Desert region termites, animals, and gas leaking are the largest sources. Metropolitan Australian emissions are dominated by animals, coal, and landfills.

[25] To compare model and TCCON XCH_4, the model is sampled at the time and location of each measurement and convolved with site-specific averaging kernels from the TCCON instruments, **A**:

$$X_{CH_4} = X_{CH_4,a} + \mathbf{a}(\mathbf{x_m} - \mathbf{x_a}), \quad (2)$$

where $\mathbf{x_a}$ is the a priori XCH_4 in the TCCON retrievals and $X_{CH4,a}$ is the associated column amount; $\mathbf{x_m}$ is the model CH_4; **a** is the column averaging kernel, given by $\mathbf{t}^T\mathbf{A}$, and $\mathbf{t}^T$ is the transpose of the column integration operator. The dominant source of variation in the instrument averaging kernels is due to change in solar zenith angle for each measurement. In the XCH_4 calculation, averaging kernels from the measurements were averaged over five-degree solar zenith angle bins. Averaging kernels at both Darwin and Wollongong are fairly uniform around one at all times of the year. Examples of kernels for a similar instrument at Lamont, in the United States, can be found in the work of *Wunch et al.* [2011].

6. Quantifying Wetlands CH_4 Fluxes in Northern Australia

[26] Emissions from wetlands are primarily driven by a positive correlation with temperature and changes in the water column [e.g., *Bloom et al.*, 2010]. In the tropics, changes in emissions are determined mainly by changes in the water table, as the temperatures are fairly constant throughout the year. To represent emissions from wetlands in northern Australia, we constructed an emissions budget using Gravity Recovery and Climate Experiment (GRACE) gravity anomaly data [*Tapley et al.*, 2004] from 2003 to 2009 at 1° × 1° horizontal resolution and a 10-d temporal resolution between 20°S and 10°S and 125°E and 150°E. The gravity anomaly is used here as a proxy for the water column. The gravity anomaly data were then interpolated to the 2° × 2.5° resolution used by GEOS-Chem. Grid boxes closer than 400 km to coast lines were omitted to minimize contamination from tides and ocean currents [*Tapley et al.*, 2004], eliminating 13 of 27 grid boxes. The coastal grid boxes were filled in using the gravity anomaly temporal variation from adjoining cells, scaled by a climatological value for wetland cover [*Kottek et al.*, 2006]. Negative gravity anomalies were replaced with zero, which assumes that when areas are drier than the mean over the measurement period of GRACE the seasonal wetlands no longer emit methane. While this need not be the case, the permanent wetland component continues emitting.

[27] We normalized the methane emission values and scaled the 2008 emissions to the total seasonal wetlands emission estimate of 0.4 Tg/year from *Deutscher et al.* [2010a]. The emissions from other years were scaled to 2008 using the ratio of the total gravity anomaly for that year, giving total emissions of 0.2 Tg/year, 0.7 Tg/year, and 0.3 Tg/year for 2005, 2006, and 2007, respectively. Over the same region constant wetland emissions (permanent wetlands from hereon in) were scaled to 0.5 Tg/year, the value found by *Deutscher et al.* [2010a].

[28] Figure 5 shows the resulting wetlands emissions in northern Australia for the time of the train campaigns. From here on in, these additional wetlands are referred to as NEWWET. The inventory created here has seasonal wetlands emissions between December and March, coincident

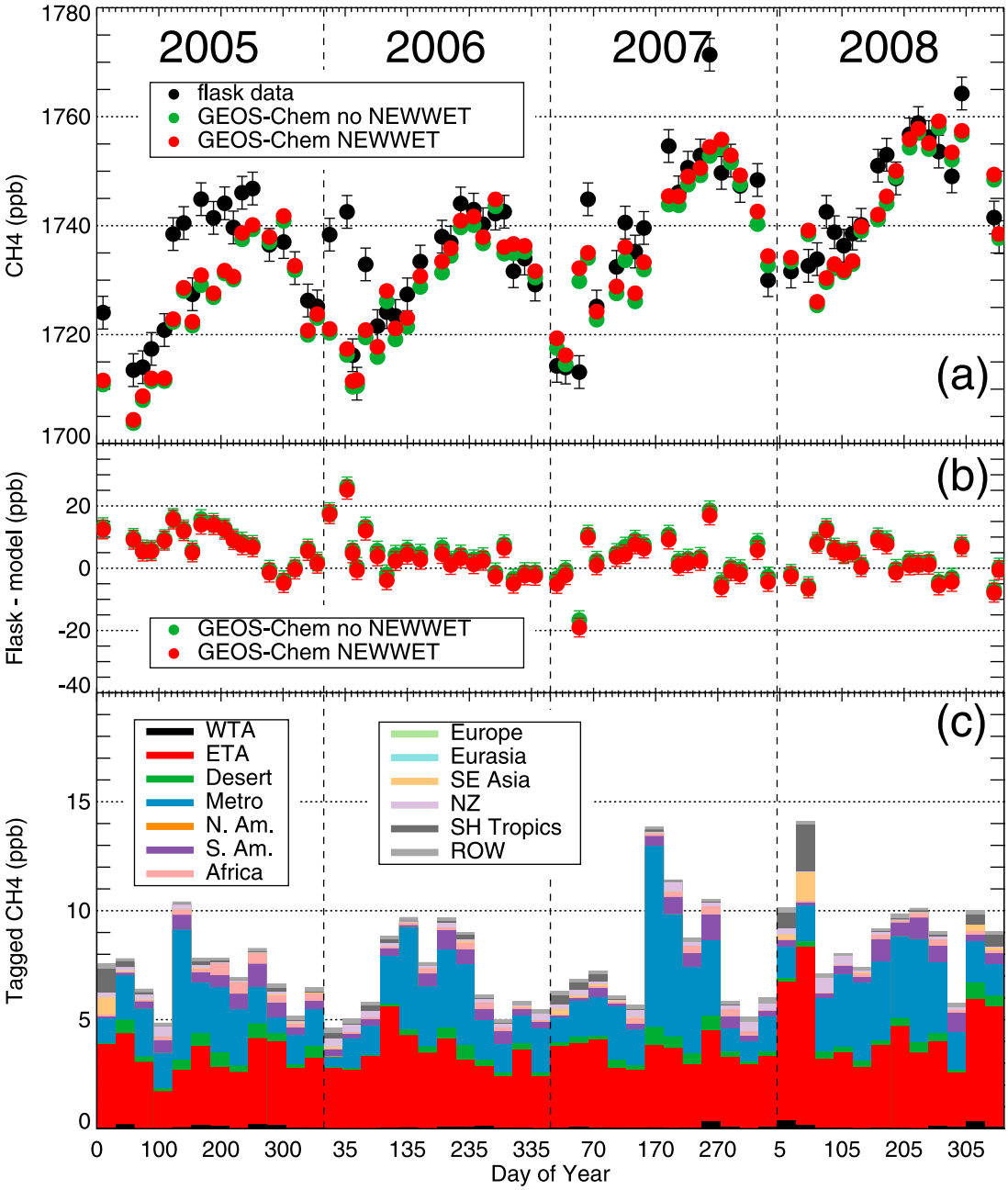

Figure 6. (a) Model and observed weekly methane surface concentrations (ppb) at Cape Ferguson (19.3°S, 147.1°E) between 2005–2008. Model results are shown with and without NEWWET. (b) Difference between observed and model concentrations. (c) Monthly mean tracer results for the 13 geographical regions. The horizontal resolution of GEOS-Chem is 2° × 2.5°. The model was sampled at the location and time of the measurements.

with the monsoonal season (section 3) when wetlands are expected to be emitting the most methane. In the dry season, the seasonal wetlands emissions are zero but the constant emissions remain.

7. Results

[29] This section discusses comparisons with the data over Australia between 2005 and 2009. A broader, more detailed evaluation of the model can be found in Appendix A, where the model is compared to ground-based flask measurements of surface concentration, aircraft-borne measurements of the upper troposphere from Civil Aircraft for the Regular Investigation of the Atmosphere Based on an Instrument Container (CARIBIC) flights, and satellite-borne measurements of the stratosphere from the Halogen Occultation Experiment (HALOE) instrument. For each comparison the model is sampled at the same location and time as the measurement.

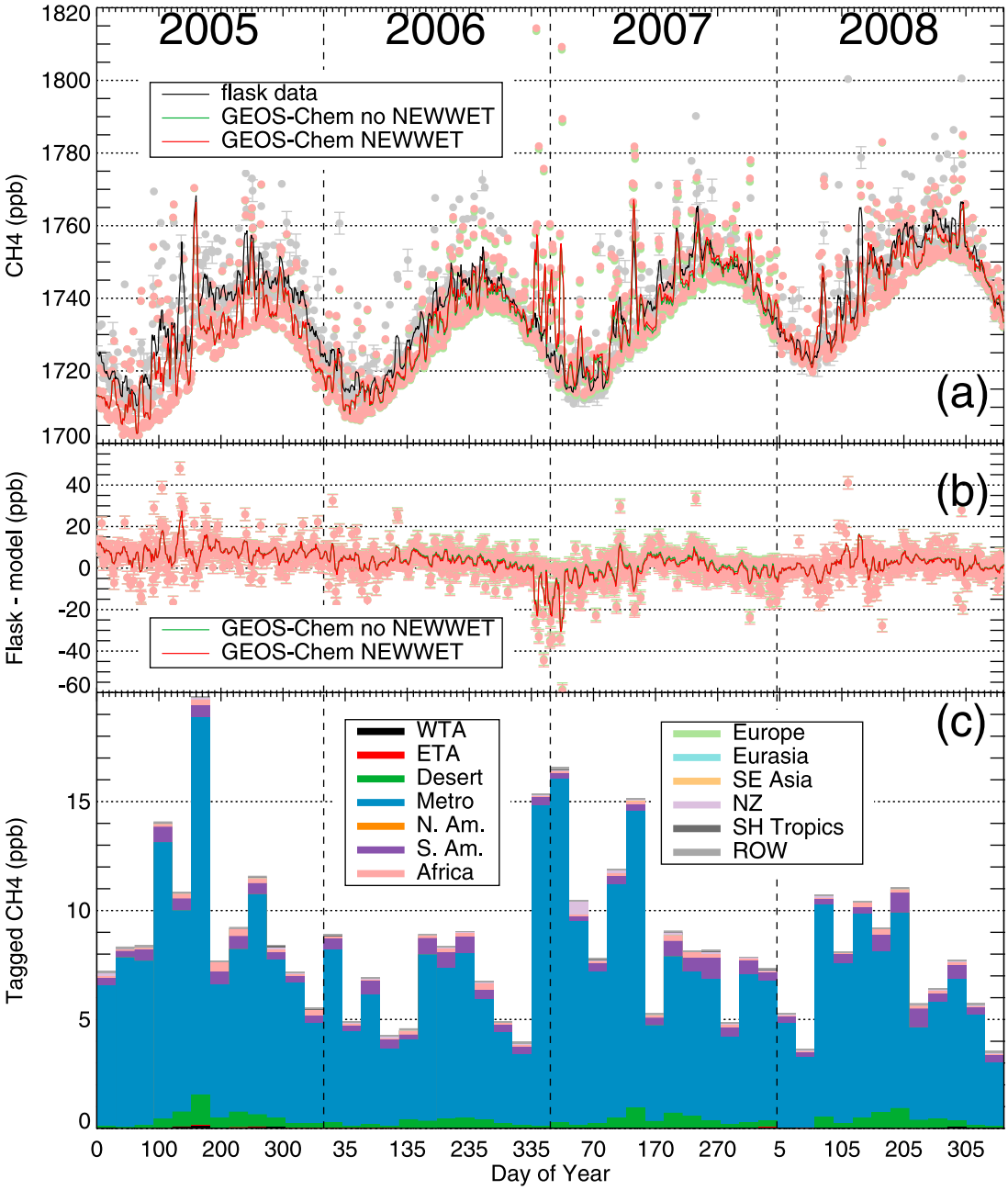

Figure 7. As Figure 6, but for Cape Grim (40.7°S, 144.7°E) and with daily resolution. (a and b) The symbols are daily-averaged measurements while the solid lines are 7-d running means.

7.1. Surface Concentrations at Flask and AGAGE Sites

[30] Figures 6 and 7 show the model and measurements of surface methane at Cape Ferguson and Cape Grim, respectively. The model output is shown both with and without NEWWET. At Cape Ferguson, surface winds are generally from the east, as discussed in section 3, so the measurements reflect clean air from the Pacific Ocean. When the winds are from the west, continental air is sampled and the concentrations are higher. The surface concentration from the model run with NEWWET is up to 3 ppb larger than the model run without, and increase the model concentration by less than the error bars of the measurements. The seasonal variation of the surface concentration is well described by the model: the correlation coefficient (r^2) is 0.75 with NEWWET and 0.74 without. The average difference between the data and the model with NEWWET is 3.6 ± 6.9 ppb (0.20%) (mean ± one standard deviation); without NEWWET the average difference is 4.8 ± 6.7 ppb (0.27%).

[31] For Cape Grim, NEWWET makes very little difference, as expected for a measurement site so far from these revised emissions. The concentrations generally reflect clean atmosphere values of methane. When the winds are from the east or north, higher concentrations reflect local emissions from Tasmania and transport in from other regions of Australia, respectively. Figure 7a shows that the model

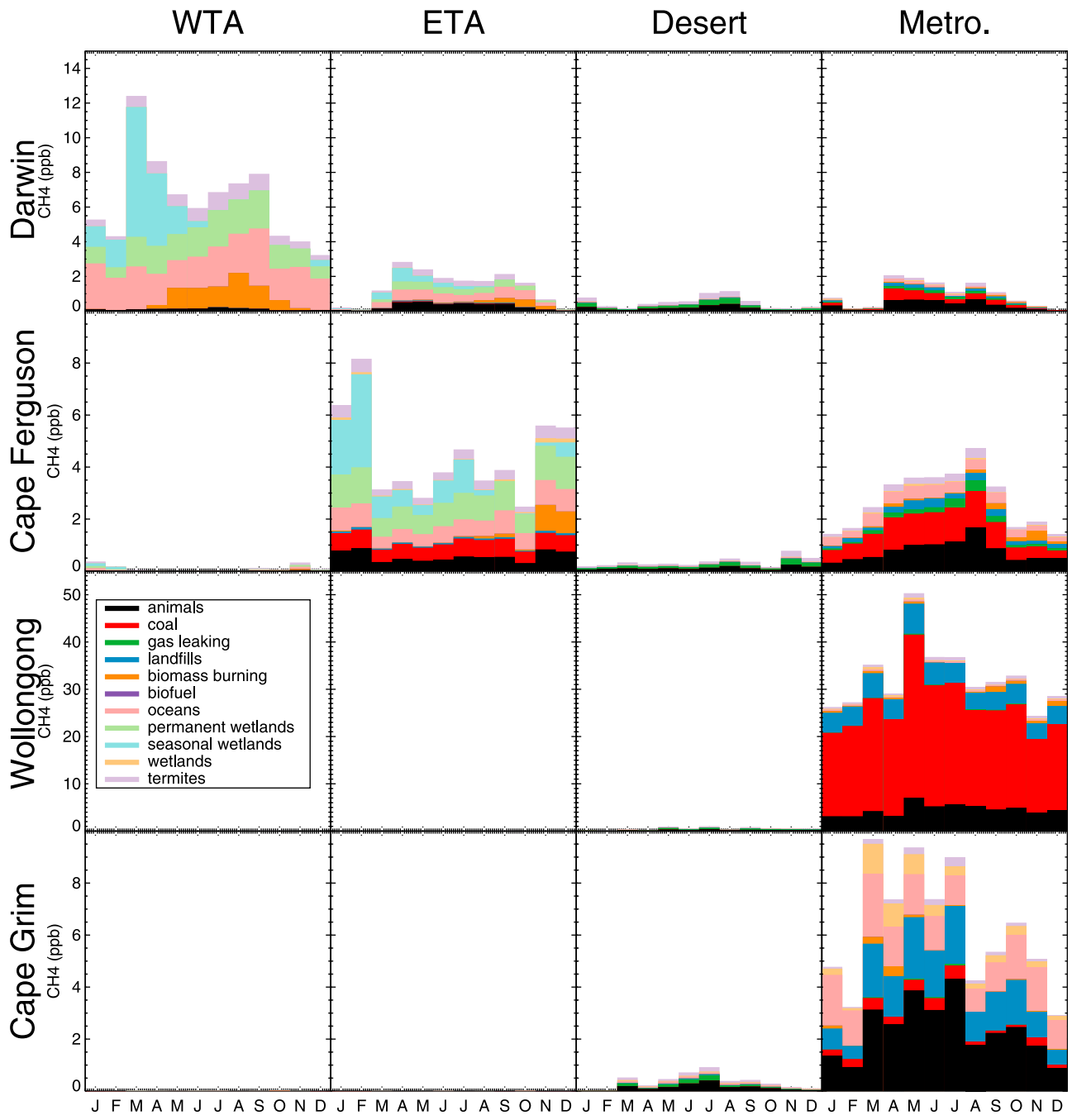

Figure 8. Model monthly averaged contribution to the surface concentration from tagged sources for Darwin, Cape Ferguson, Wollongong, and Cape Grim. From left to right the columns show contributions from West Tropical Australia (WTA), East Tropical Australia (ETA), Desert Australia, and Metropolitan Australia. Note the different y-axis scales for the different sites. Permanent and seasonal wetlands are NEWWET emissions in northern Australia, while wetlands are located mainly in the southeast of the country.

reproduces the background concentrations well, but has difficulty reproducing concentrations influenced by local sources: the model both underestimates and overestimates these elevated events. The mean difference between the data and the model is 3.1 ± 8.4 ppb (0.15%) with a correlation coefficient of 0.74.

[32] At both sites, the model slightly overestimates the growth rate of methane. There is a trend of −2 ppb/year in the difference between the data and the model. A similar trend is seen at other surface flask sites (see Appendix A). The trend is likely due to an overestimation in the increase of anthropogenic emissions in the model.

[33] Figures 6 and 7 also show the monthly mean contribution to surface concentration above background from the geographic tagged tracers with NEWWET. As discussed in section 5, the tagged tracers were set to zero at the beginning of each month with previous monthly contributions subsumed by the background tracer. Figure 8 shows

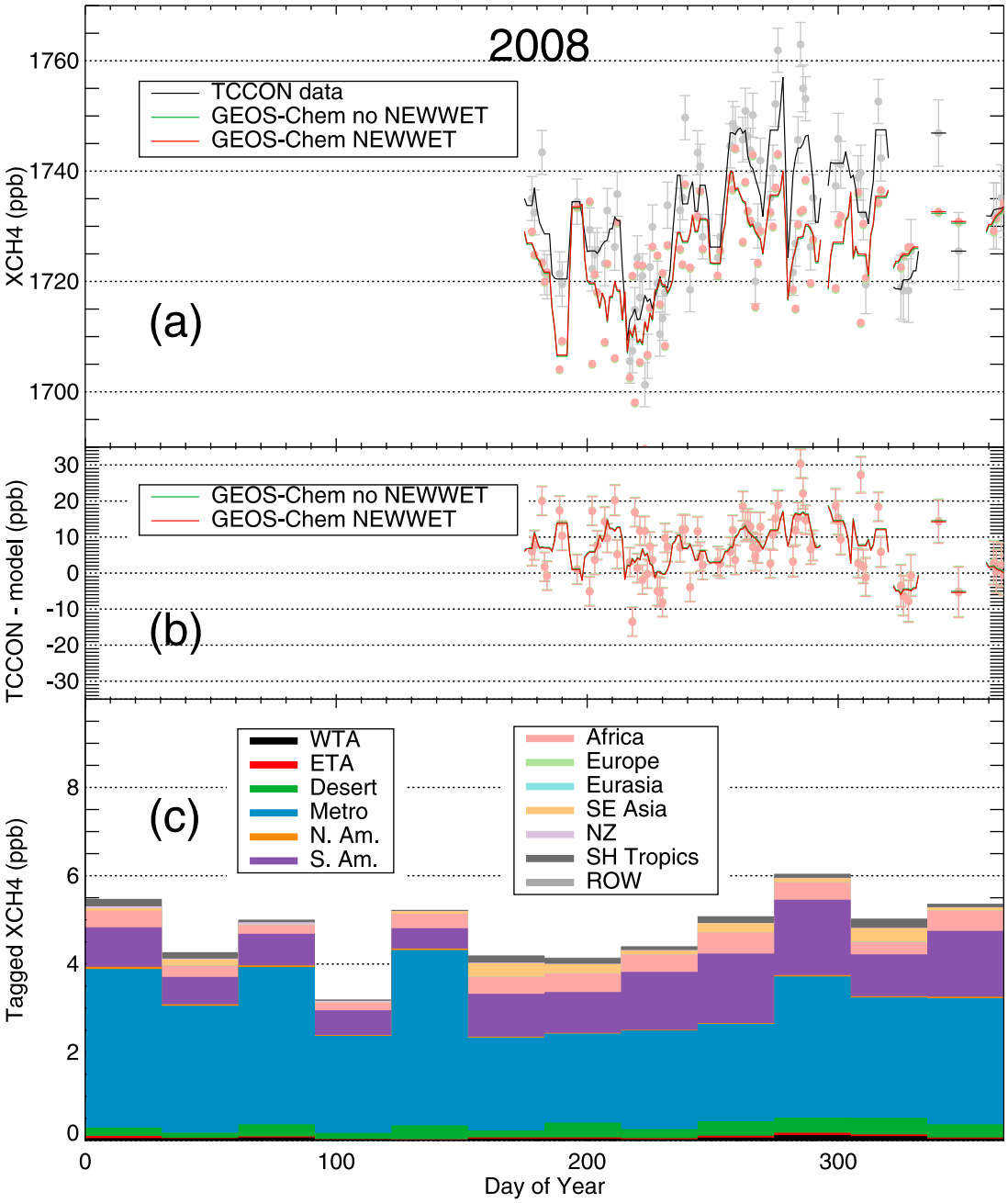

Figure 9. (a) Model and TCCON total column daily methane at Wollongong (34.4°S, 150.9°E). The two model results are with and without the new wetland emissions. (b) Difference between TCCON measurements and model output. The symbols represent the daily averaged measurements while the solid lines represent a 7-d running mean. (c) Monthly mean tracer results.

the monthly-averaged contributions to the surface concentration above background from the different sources for the four Australian regions from the tagged tracer run for 2008.

[34] At Cape Ferguson, the change to the surface concentration above background is about equally influenced by local emissions (25–60%) and transport from the Metropolitan Australian region to the south (10–60%). The local emissions are from oceans, NEWWET, animals, and coal. These sources are constant throughout the year with the exception of the seasonal wetlands, which are strongest in the summer. Emissions from Metropolitan Australia are dominated by coal and animals and their influence at Cape Ferguson is largest in the autumn and winter, reflecting general circulation patterns (section 3). The relative contribution of the sources is similar from year to year (not shown), except in the case of seasonal wetlands, which are much stronger in 2006 and 2008. Transport from South America and Africa is the largest intercontinental contribution, the effects of which peak in the winter and early spring. There is also transport from Southeast Asia and the Southern Hemisphere tropics in the summer, with the largest effect in 2008 (5 ppb).

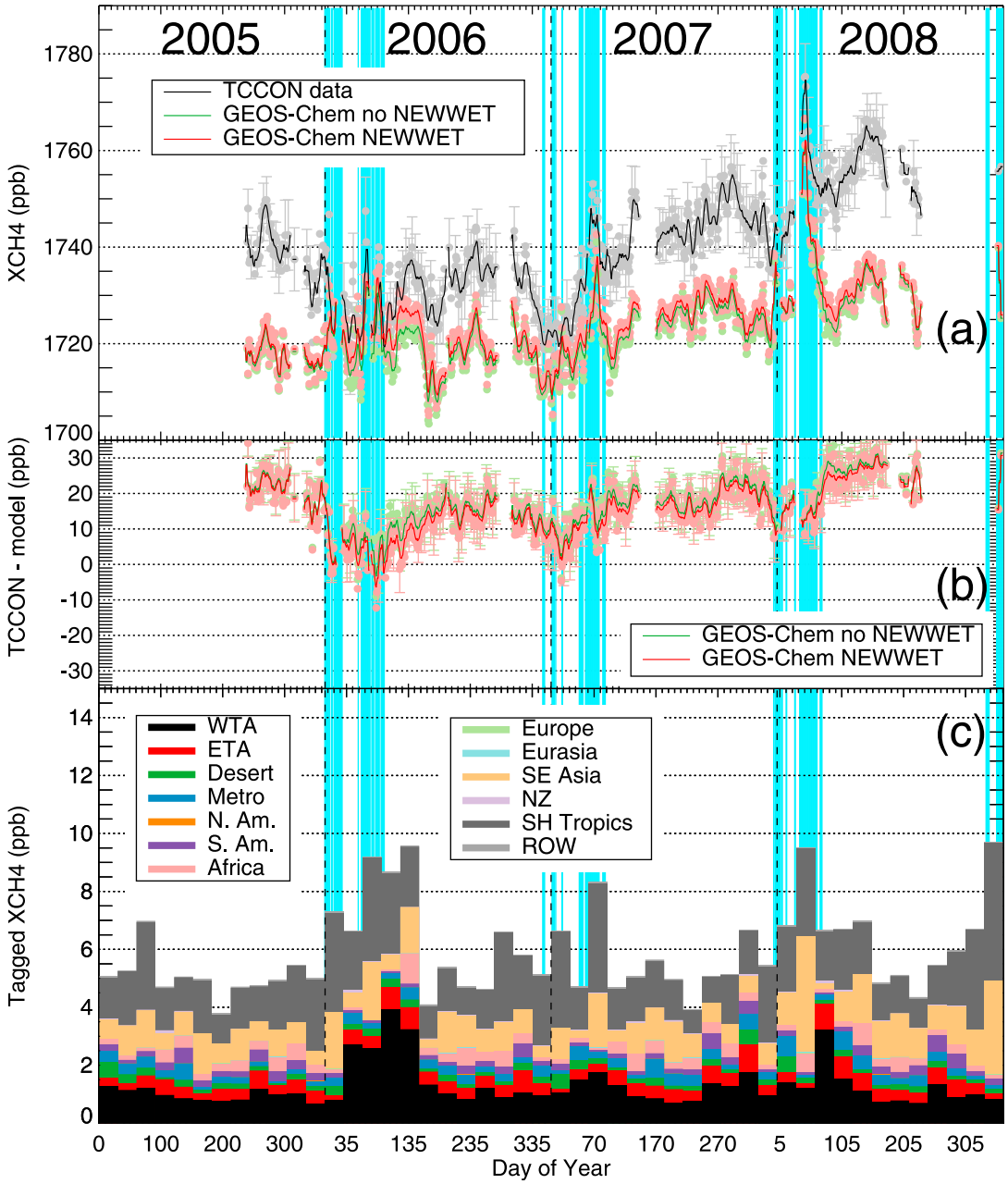

Figure 10. As Figure 9, but for Darwin (12.4°S, 130.9°E). The blue shaded regions represent times when Darwin is in the chemical Northern Hemisphere (see text).

[35] At Cape Grim, local emissions from animals, landfills, and wetlands (located in southern Victoria and South Australia) are the largest contributors to changes in the surface concentrations above background (75–95%). Contributions from biomass burning are largest in the autumn, while contributions from wetlands are largest in the summer and autumn (December–June). There is interannual variability in contributions from biomass burning, which is largest in 2007, and wetlands, which are largest in 2005. The spike in the tracers in late 2006/early 2007 is caused by a large biomass burning event, where large methane values are seen in the model but are not observed in the data. Transport into the region from overseas is primarily from South America and Africa and is strongest in the winter and spring, similar to Cape Ferguson.

7.2. XCH_4 at TCCON Sites

[36] Figure 9 shows the model and measured XCH_4 at Wollongong. Including wetlands emissions from northern Australia makes very little difference to the columns, as expected. The TCCON instrument at Wollongong began operating in 2008, so the record is not as long as for the surface sites. The model and data agree well: the mean difference between the data and the model is 7.1 ± 8.4 ppb (0.40%) and a correlation coefficient of 0.60. These comparisons are consistent with the model comparison of surface concentration comparisons at Cape Ferguson and Cape Grim.

[37] Figure 9c shows the monthly mean tracer results for the total column above background at Wollongong. The XCH_4 is dominated by emissions from the Metropolitan

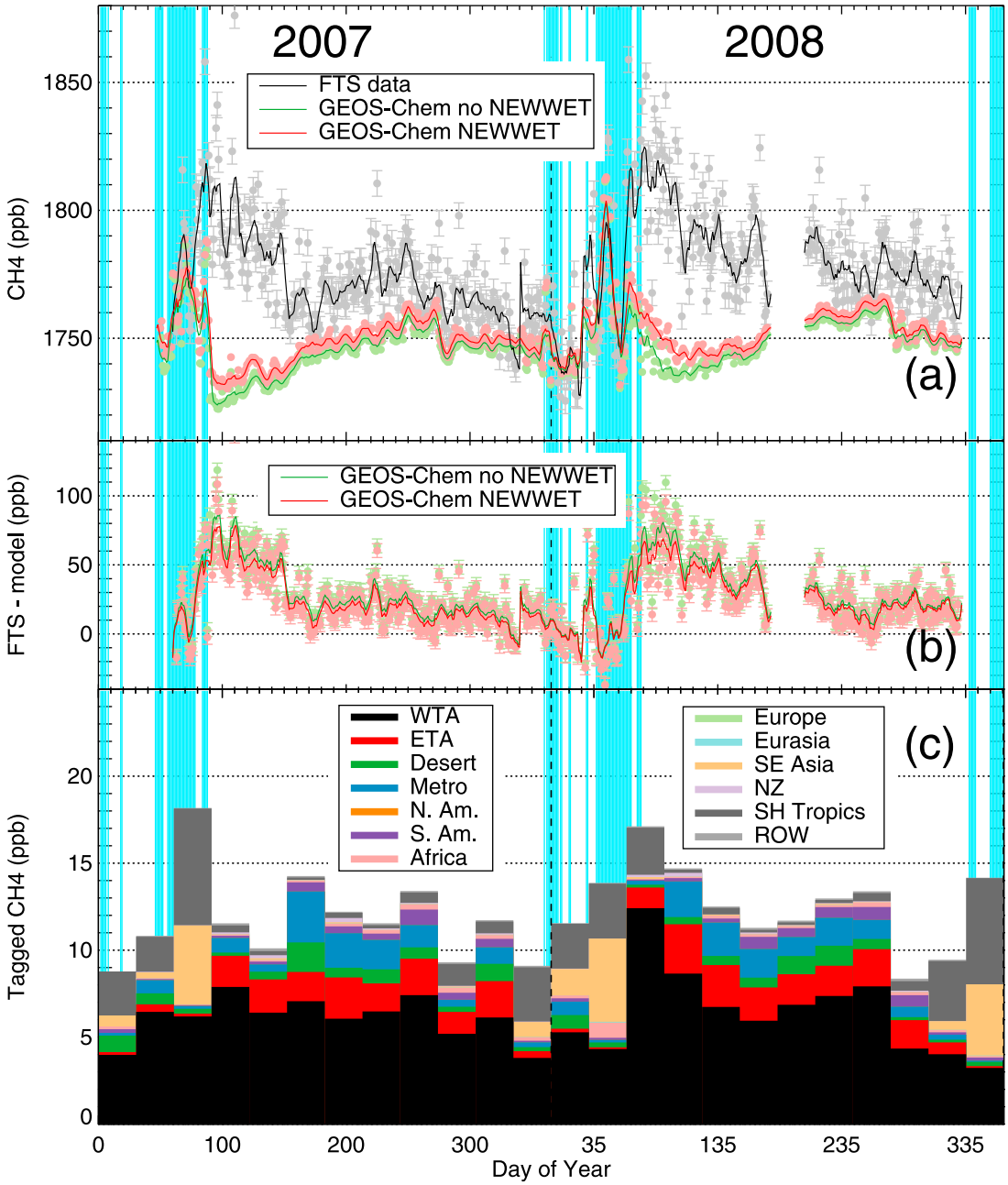

Figure 11. As Figure 10, but for surface CH_4.

Australian region. Figure 8 shows that at the surface emissions from coal mining are the dominant contribution to the change in concentration above background (90–95%), with only small contributions from animals, landfills, and biomass burning. Transport from South America, strongest in winter and spring, is the second largest source of additional methane above background at Wollongong.

[38] Figure 10 shows the XCH_4 at Darwin. The difference between the model run with and without NEWWET is up to 8 ppb and is largest in the summer when the seasonal wetlands are active. However, the prevailing winds at this time of year are from the north and west, while the bulk of the seasonal wetlands lie to the south, so it is not expected that NEWWET will have a great effect at Darwin. The blue shaded regions indicate periods when Darwin is located in the meteorological northern hemisphere. A GEOS-Chem simulation of an idealized inert tracer was used to determine the position of the chemical gradient formed due to the ITCZ associated circulation; this is further discussed in Appendix B. The mean difference between the data and the model is 15.9 ± 7.5 ppb (0.91%) with NEWWET and 17.4 ± 7.2 ppb (0.99%) without.

[39] During the periods when Darwin is in the chemical Northern Hemisphere, the model reproduces the data well (r^2 = 0.76, increasing to 0.87 if only 2007 and 2008 are considered). Outside of these periods, the model tends to have a negative bias with respect to the data (peaking at 34 ppb in 2005 and 2008). The model shows a larger drop

off than the data when the chemical equator moves northward away from Darwin, perhaps indicating that the motion of the chemical equator is a more gradual process in time than described by the GEOS meteorological fields. It is also possible that there is a missing source, or a source that is underestimated in the model, outside of Australia. This would cause the model to underestimate the methane column when transport over Darwin is from that region. The difference between the data and the model shows a seasonal cycle, with minima during the summer months when the chemical equator lies to the north. During this time period, the prevailing winds at Darwin are from the north, while at other times of year the winds are predominantly from the south and east. Generally, the model reproduces the day-to-day variability in methane but not the overall trend. The modeled methane increases by about 5 ppb/year over the 3.5 year data record, while the data increases by about 8 ppb/year over the same time period.

[40] Figure 11 shows the model and measured surface CH_4 at Darwin from a ground-based in situ FTS colocated with the TCCON instrument. The seasonal cycle in the residuals in both the surface data and the total column data is at a minimum during the Northern Hemisphere intrusions. Right after the intrusions, both increase. In the total column the residuals continue to increase throughout the dry season and decrease as the wet season begins again. At the surface, the residuals decrease through the year.

[41] Figures 10c and 11c show the monthly mean geographical tracers at Darwin, while Figure 8 shows the surface concentration tracers from the Australian regions broken down into sources. Intercontinental transport is stronger in the total column, reflecting that sources are emitted at the surface, whereas intercontinental transport into the region mainly occurs in the free troposphere. Emissions from the local region are the largest contributors to the concentrations above background at the surface. These are comprised of oceans, NEWWET, and biomass burning. The seasonal wetland source is largest in the wet season, when the wetlands are active, as expected. Emissions from biomass burning are larger in the dry season. Local emissions contribute 30–75% of the change to the surface concentrations above background and 10–50% of the added total column. Transport from Southeast Asia and the Southern Hemisphere tropics make comparable contributions to the total column in spring and summer, during the Australian-Indonesian monsoon. The relative contribution of the sources is similar from year to year, except in the case of seasonal wetlands, which are much stronger in 2006 and 2008.

[42] The behavior of the residuals between the model and measured concentrations at the surface and in the total column together with the tracers suggest reasons for the model-measurement discrepancy. In the first half of the year the residuals behave similarly, pointing to a common cause of the discrepancy. At this time of year, both surface and total column tagged tracers are dominated by local emissions from the West Tropical Australia region (mainly NEWWET) and transport from Southeast Asia and the SH Tropics. In the second half of the year, the residuals behave differently from one another. The total column tracers show greatest influence from transport from SE Asia and the SH Tropics, while the largest local source emitted in the region is biomass burning. The surface tracers are mostly biomass burning and ocean emissions from West and East Tropical Australia. The influence of transport from the Desert and Metropolitan regions for both the total column and surface concentrations is largest during the second part of the year. This suggests that at the surface, the emissions from the tropical regions of Australia are underestimated. The measurements of the total column are more affected by transport than measurements at the surface, which indicates an underestimated source lying north of Australia, or a source underestimated in the Desert or Metropolitan region.

7.3. Surface Concentrations Along the Ghan Train Route

[43] Figure 12 shows the hourly averaged ground-level methane concentrations measured by the in situ FTS installed on the Ghan train for the three campaigns held in 2008. Error bars on the measurements represent the standard deviation of the measurements over the hour. Local emissions contaminate the concentrations when the train stops in the cities of Alice Springs (23.7°S), Katherine (14.5°S), and Darwin (12.4°S), indicated by the vertical grey lines in Figure 12, and are not expected to be reproduced by the model.

[44] For all campaigns, the concentrations of methane gradually increase as the train moves northward into the tropics with a latitudinal gradient of 1.2 ± 0.2 ppb/degree latitude [*Deutscher et al.*, 2010a]. The model latitudinal gradient of methane is 1.1 ± 0.3 ppb/degree latitude and 0.4 ± 0.2 ppb/degree latitude for the model with and without NEWWET, respectively. Without NEWWET, the model does not capture the increase in methane as the train moves northward toward the equator.

[45] Figure 13 shows results from the tagged tracer GEOS-Chem for the model run with NEWWET, which gives the source region for the change in methane concentration above background. The colored vertical lines indicate when the train moves from one region to another. The largest source in any given region is local sources from within that region, with influence from adjacent regions at the boundaries.

[46] Qualitatively, the model with NEWWET agrees with the data better than the model without, but some systematic lack of agreement remains. Some of the individual discrepancies could be due to the relatively coarse resolution of the model (2° × 2.5°). For all campaigns, NEWWET does not significantly affect the concentrations south of 20°S, as expected, where the model overestimates the concentrations by roughly 10 ppb for the first two campaigns and 0–20 ppb for the third.

[47] For the first campaign in February, the data and both of the model runs show an increase in methane concentration moving northward. In the model this is partly due to an intrusion from the Northern Hemisphere, as indicated by the influence from Southeast Asia in Figures 13a and 13b. North of 15°S the model with NEWWET and the data agree within error bars, while south of this the model overestimates the concentrations. For the northbound portion of this campaign, the model is 10–60ppb higher than the data in this region. Figure 13a shows that the overestimation of the concentration is due to emissions from the Western Tropical region of Australia, the majority of which is from seasonal wetlands. Owing to the gap in data between 16° and 18°S,

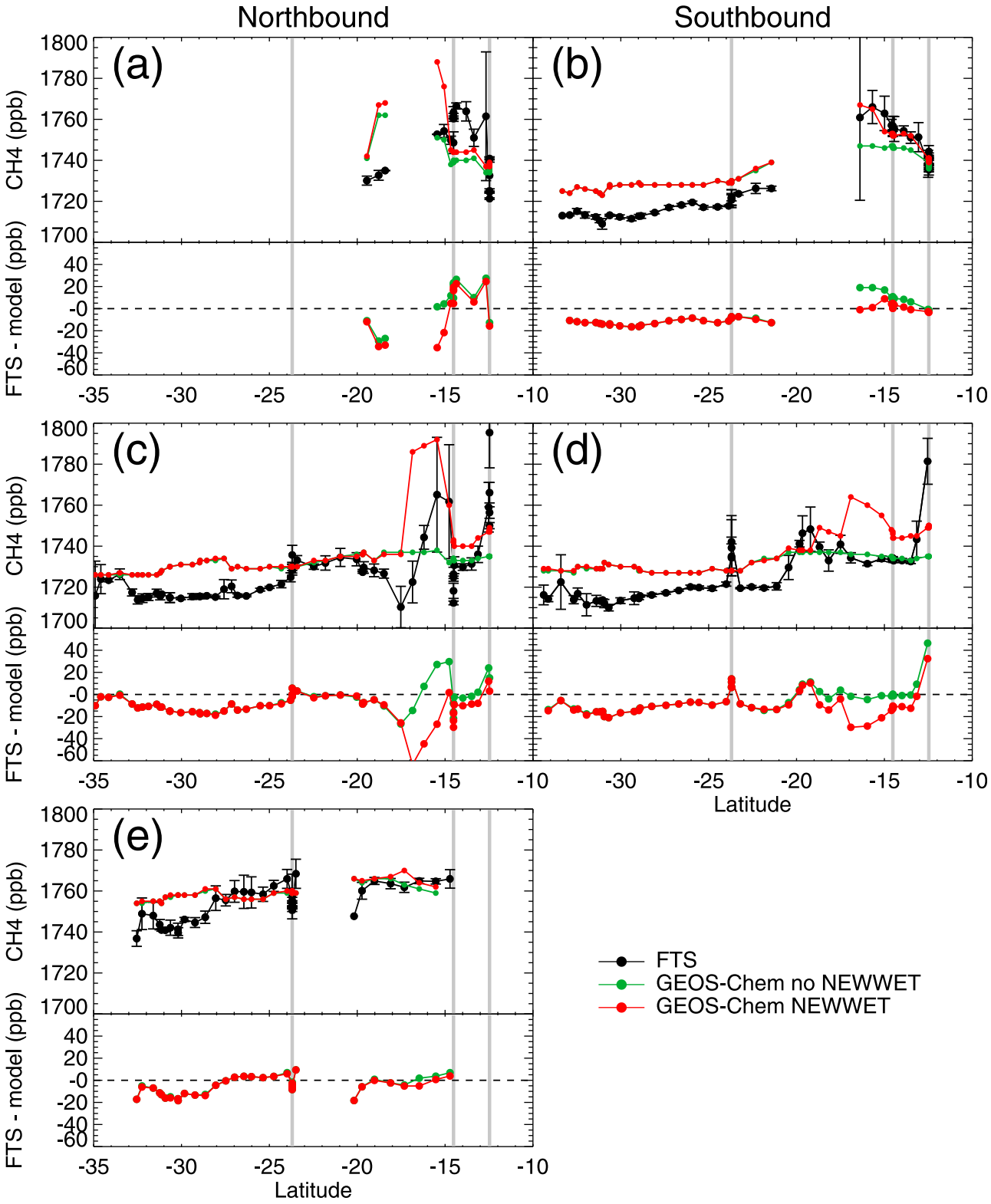

Figure 12. Hourly averaged model and observed methane concentrations for the three Ghan train trips in (a–b) 26–29 February, (c–d) 30 March to 4 April, and (e) 28–30 September 2008, showing (left) northbound and (right) southbound trips. Error bars represent the standard deviation of the measurements. The GEOS-Chem model concentrations are shown with and without NEWWET. In Figures 12a–12e the difference between the data and the model is shown at the bottom. The vertical grey lines indicate the locations of Alice Springs (23.7°S), Katherine (14.5°S), and Darwin (12.4°S).

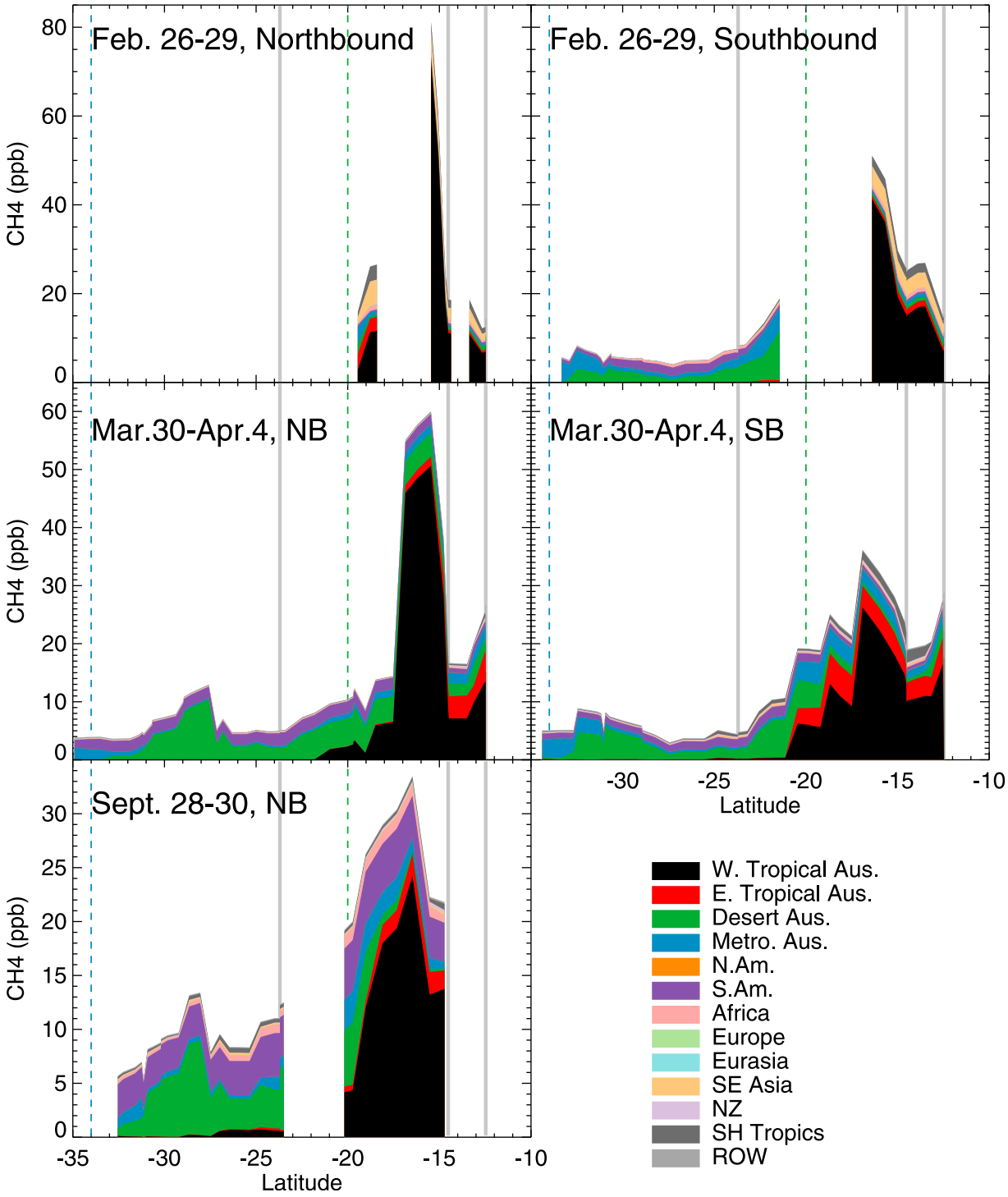

Figure 13. As Figure 12 but for tagged tracer concentrations. The vertical colored lines indicate the transition between the Metropolitan Australian region and the Desert region (blue) and between the Desert region and the West Tropical region (green).

where the model begins to see an increase in the methane concentrations, it is difficult to draw conclusions from this portion of the campaign. The mean difference between the data and the model for the entire campaign is −7.4 ± 10.8 ppb (−0.43%, RMS difference 11.7 ppb) without NEWWET, improving to −4.8 ± 7.0 ppb (−0.28%, RMS difference 10.1 ppb) with NEWWET.

[48] During the second campaign in March, the chemical equator was to the north of Darwin, and the entire train trip took place in the chemical Southern Hemisphere. This is confirmed by Figures 13c and 13d, which show very little influence from Southeast Asia but some influence from the Southern Hemisphere Tropics. Transport from other regions of Australia plays a larger role, indicating that the shift in

surface winds associated with the end of the monsoon has occurred. The mean difference between the data and the model with NEWWET is −5.3 ± 11.3 ppb (−0.31%, RMS difference 12.3 ppb) and −10.0 ± 11.5 ppb (−0.58%, RMS difference 15.2 ppb) without them.

[49] For the northbound portion of the second campaign, the model displays a positive bias south of Alice Springs. North of this, the model and data agree within error bars until 20°S, where the data show a large increase in methane concentrations. This is roughly reproduced by the model with NEWWET, but is absent in the model without these emissions. Figure 13c indicates that this increase is caused by emissions from West Tropical Australia, which are dominated by emissions from the seasonal wetlands. In the southbound portion of the campaign, the peak in the data at roughly 20°S is caused by a local biomass burning event not included in the GFED emissions used in the model; as a result the model is not expected to reproduce this peak. North of this, the model without NEWWET agrees with the data within error bars, while the model with NEWWET remains about 10–15 ppb larger than the observations.

[50] For both of these campaigns, south of Alice Springs, the methane concentration is more constant, and the influence of the tagged tracers is small. Near Adelaide (34.9°S), emissions from Metropolitan Australia dominate. As the train moves further north into the Desert region, local emissions from this region and transport from South America are the largest contributors to the signal above background. The difference between the model and the data are most correlated to the local emissions from the Desert region (r^2 ranging from 0.12 to 0.61). Emissions in this region are dominated by animals and termites. In the model, emissions from both sources are assumed to be constant throughout the year. Emissions from ruminant animals vary from year to year and are scaled to match the estimates from the Australian NGGI. Emissions from termites are known to vary with temperature and water availability, and possibly the model bias in this region could be a result of interseasonal variation in these sources that are not described by the model. The soil sink, which is treated as a constant in the model, could also vary with time. It is also possible that the soil sink is underestimated in the model, which could explain the positive bias in the model surface methane concentrations. In the same region there is little correlation between the model minus the measurements and the long-range transport tracers, suggesting the model describes the transport accurately. North of 20°S, the differences between the model and data are mainly due to NEWWET. This indicates that the seasonality and magnitude of the wetlands emissions is more complex than the seasonality of the gravity anomaly from GRACE, which we expect. Wetlands emissions vary not only with the water column and the temperature but also with other factors such available soil carbon and soil salinity.

[51] The third campaign took place during the dry season in September, and there are no emissions from seasonal wetlands during this time. Only the permanent wetland emissions are different between the two model runs, and as a result both runs are mostly similar. The model is roughly 20 ppb higher than the data south of 28°, but generally reproduces the gradient seen in the observations. The mean difference between the data and the model with NEWWET is −4.8 ± 7.8 ppb (0.27%, RMS difference 9.1 ppb) and −5.4 ± 7.6 ppb (0.31%, RMS difference 9.2 ppb) without them.

[52] Figure 13e indicates that the latitudinal gradient during this campaign is again a result of emissions from the West Tropical Australia region, here dominated by termites. As for the second campaign, there is very little influence from the northern hemisphere. Transport from South America is the second largest source when the train is in both the Desert region and the West Tropical region, consistent with the larger influence from these regions seen in the surface and column data. For this campaign, there is no strong correlation between the difference between the data and the model and any of the emissions or transport tracers, indicating that the overestimation is not dominated by any one source.

8. Discussion and Concluding Remarks

[53] We have used the GEOS-Chem model to investigate the Australian methane budget from 2005 to 2008 at four measurement sites: Darwin, Cape Ferguson, Wollongong, and Cape Grim and along the Ghan train route, which runs between Adelaide and Darwin. We have constructed a wetlands emissions map for northern Australia using gravity anomaly data from the GRACE satellite. These emissions have qualitatively improved comparisons between surface concentrations of methane taken from an FTS located on the Ghan train and the GEOS-Chem model, but systematic differences still remain. Since 2008, four more campaigns have been held, which will help to refine the seasonality, spatial distribution, and magnitude of NEWWET.

[54] We compare the model concentrations to surface data taken from measurements at Cape Ferguson and Cape Grim. The model is able to reproduce the seasonality of the data (r^2 = 0.75 and 0.74, respectively) but overestimates the growth rate in methane between 2005 and 2008 by ~2 ppb/year, which is likely due to overestimating the increase in anthropogenic emissions. We also compare the model to XCH_4 from TCCON instruments at Wollongong and Darwin. At Wollongong the model reproduces the data reasonably well (r^2 = 0.60), and consistent with the trend seen at Cape Ferguson and Cape Grim. At Darwin, the model reproduces the daily variations in XCH_4. The model agrees with the Darwin data in the wet season when the location is in the chemical Northern Hemisphere (r^2 = 0.76, improving to 0.87 if only 2007 and 2008 are considered) but underestimates the column in the dry season.

[55] The differences in both the surface concentration and total column at Darwin indicate missing processes in the model. The source of the discrepancy is likely not a result of an underestimation of NEWWET, a 1 Tg local source to Darwin, which increases the total column there by at most 8 ppb, while the differences between the measurements and model are up to 20 ppb. As confirmed by the general agreement seen between the model and the measurements from the Ghan train, the magnitude of NEWWET is approximately correct, and it is unlikely that the magnitude of this source should be three times larger. The variation of methane with respect to the location of the chemical equator in the wet season and soon after suggest a negative bias in the interhemispheric transport of the model. The behavior of

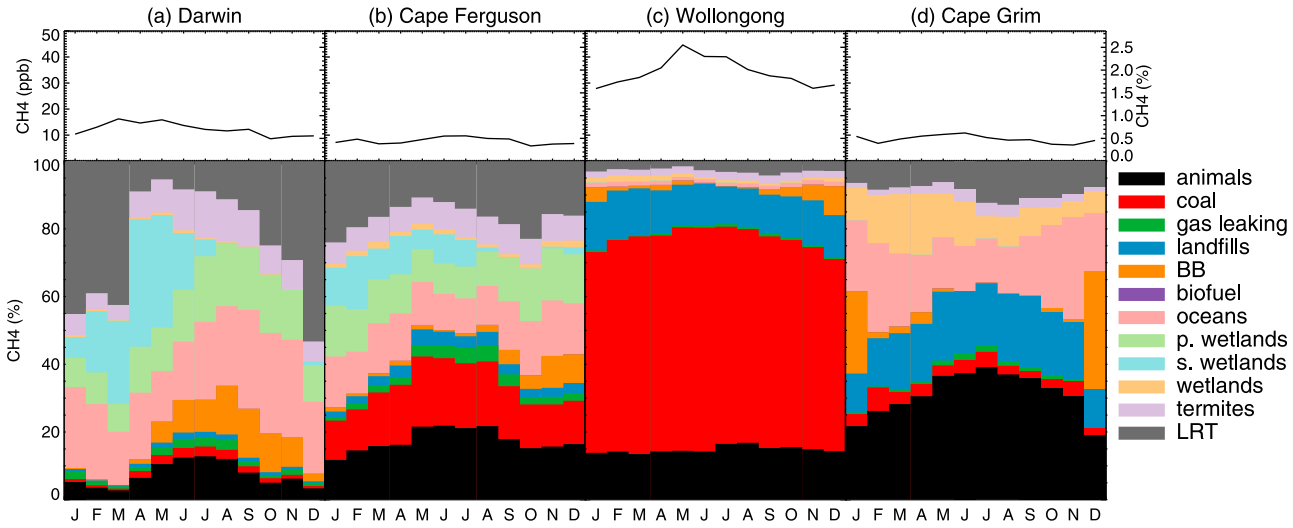

Figure 14. (top) Mean of the total of the tagged tracers in ppb and as a percent of the total tracer including the background term for (a) Darwin, (b) Cape Ferguson, (c) Wollongong, and (d) Cape Grim. (bottom) Contribution to the surface monthly mean methane concentrations.

the residuals between the surface and total column measurements in the dry season suggest a missing source, or a source that is underestimated, outside of Australia, most likely to the north.

[56] We used the model to identify the relative importance of local sources and long range transport at the four stationary sites and along the Ghan train route. Figure 14 summarizes the budget from the model for the TCCON and surface sites and gives the mean of the total of the tagged tracers for the 4 years studied here. The smaller value of the total tagged tracer at Cape Ferguson and Cape Grim reflect their status as clean air sites, while the large value at Wollongong reflects its proximity to urban areas and the Southern coalfields. This figure also shows the monthly mean percentage contribution to the change in concentration above background at the four observation sites averaged over 2005–2008. At Cape Ferguson, Wollongong, and Cape Grim, local sources and intracontinental transport have the largest effect on the change in concentrations, with long-range transport accounting for no more than 25% of the signal above background. The concentrations at Darwin are influenced by transport from tropical regions to the north of Australia, and during the monsoon season intercontinental transport can account for 50% of the change in surface concentration above background.

[57] Annual mean contributions to the total tagged tracer are given in Table 3. At Darwin, Cape Ferguson, and Cape Grim, emissions from ruminant animals are the largest anthropogenic source. At Wollongong, emissions from coal are the largest source. Annually, oceans are the largest natural source at Darwin, Cape Ferguson, and Cape Grim, while termites are the largest natural source at Wollongong. This reflects the coastal location and mean air flow at the first three sites and the continental airflow at Wollongong. This is also seen in the contribution from long-range transport, the effect of which is smallest at Wollongong.

[58] Measurements from the Ghan train suggest interseasonal variability in the emissions from ruminant animals

Table 3. Mean Contribution of the Source Tracers and Long-Range Transport to the Total Tagged Tracers for the Four Measurement Sites From 2005 to 2008

	Darwin				Cape Ferguson				Wollongong				Cape Grim			
	Surface		Column		Surface		Column		Surface		Column		Surface		Column	
Source	ppb	%	ppb	%	ppb	%	ppb	%	ppb	%	Ppb	%	ppb	%	ppb	%
Anthropogenic Sources																
Ruminant animals	0.92	7.4	0.31	5.4	1.39	17.5	0.36	8.6	5.05	14.8	0.90	17.9	2.67	31.3	0.45	16.6
Coal mining	0.21	1.7	0.07	1.2	1.25	15.8	0.25	6.2	21.34	62.4	1.46	29.4	0.30	3.6	0.09	3.4
Gas leaking	0.21	1.7	0.08	1.3	0.23	2.8	0.10	2.5	0.20	0.6	0.09	1.8	0.08	0.9	0.06	2.3
Landfills	0.13	1.0	0.04	0.8	0.25	3.1	0.09	2.1	4.26	12.6	0.43	8.6	1.45	17.0	0.23	8.4
Biomass burning	0.77	6.6	0.19	3.6	0.21	2.9	0.08	1.9	0.69	2.2	0.13	2.4	0.50	5.9	0.07	2.5
Biofuel burning	0.00	0.0	0.00	0.0	0.00	0.0	0.00	0.0	0.01	0.0	0.00	0.0	0.00	0.0	0.00	0.0
Natural Sources																
Oceans	2.67	22.4	0.52	8.7	1.03	13.6	0.24	5.8	0.39	1.2	0.10	1.9	1.56	19.2	0.14	5.0
Permanent wetlands	1.69	13.9	0.34	5.8	0.94	12.4	0.15	3.7	0.01	0.0	0.01	0.3	0.00	0.0	0.01	0.3
Seasonal wetlands	1.74	11.9	0.39	5.9	0.49	6.1	0.11	2.8	0.00	0.0	0.01	0.2	0.00	0.0	0.00	0.2
Wetlands	0.05	0.4	0.02	0.3	0.11	1.4	0.02	0.6	0.37	1.1	0.10	2.0	0.91	10.4	0.10	3.6
Termites	1.08	8.8	0.30	5.1	0.60	7.7	0.19	4.6	0.72	2.1	0.18	3.7	0.22	2.6	0.10	3.7
Long-range transport	2.85	24.3	3.69	61.9	1.27	16.7	2.52	61.2	0.95	2.8	1.59	31.8	0.75	9.1	1.48	54.0

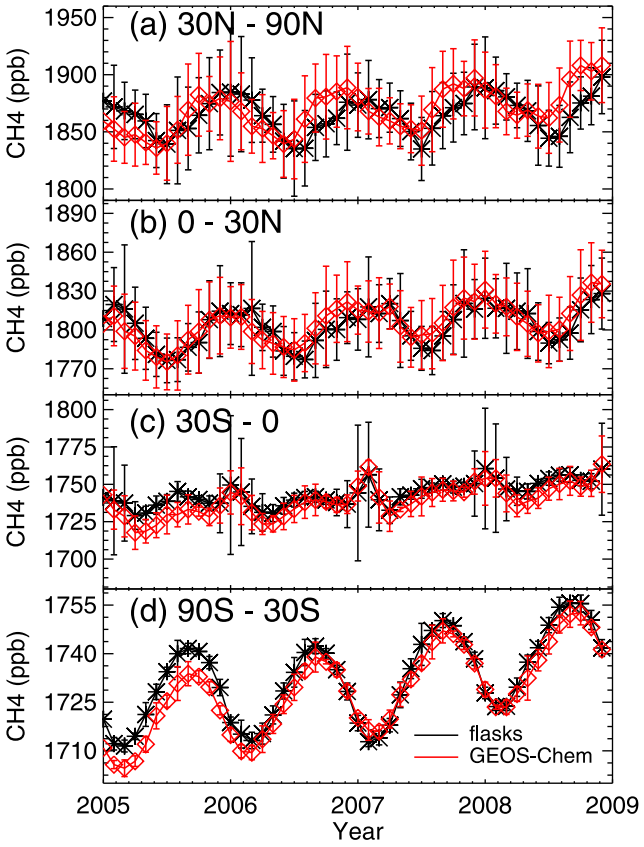

Figure A1. Monthly mean time series of weekly and hourly flask data and GEOS-Chem model output for sites between (a) 30°N and 90°N (29 sites), (b) 0° and 30°N (11 sites), (c) 30°S and 0° (eight sites), and (d) 90°S and 30°S (nine sites). The model has been sampled at the time and place of the measurements. The error bars denote the standard deviation of the monthly means at the different sites. The horizontal resolution of the model is 2° × 2.5°, and the model was sampled at the same time and location as the data.

and termites, which is not accounted for the model. The model is able to reproduce the measurements, with a mean difference of 4.3 ± 11.6 ppb over the three campaigns. The tagged tracer model identifies the source of methane along the train route and clearly shows the transitions between the urban region of Adelaide, the desert of the center of the country, and the tropical region surrounding Darwin.

[59] To the best of our knowledge, this is the first attempt to investigate the complete budget of methane including both anthropogenic and natural sources and intercontinental transport at Australian measurement sites. The emissions inventories used are able to reproduce the measurements at the clean air sites of Cape Ferguson and Cape Grim and at the coastal site of Wollongong. At Darwin, the model-measurement comparisons indicate an issue with the inter-hemispheric transport of the GEOS-Chem model, and a missing source. Along the train route, the comparisons suggest interseasonal variability not included in the emissions inventories. The wetland emissions inventory constructed here qualitatively improved the comparisons between the model and measurements, but these emissions can be further refined. More measurements in continental Australia would help to more accurately describe the sources of methane in Australia.

Appendix A: Model Evaluation

A1. Surface Sites

[60] Forty-four in situ flask monitoring stations with data spanning 2005–2008 were selected to evaluate the performance of the model at simulating surface concentrations. Sites known to be heavily influenced by local emissions were not used, since the model is not expected to reproduce these sites due to its relatively coarse resolution.

[61] Figure A1 shows the monthly mean surface concentrations from the flasks and GEOS-Chem averaged over four latitude bands. The error bars represent one standard deviation of the variation between sites. In all latitude bands the general agreement is similar to the flask sites examined in section 7.1: the model reproduces the absolute concentration of methane but overestimates the positive trend over the four year period (r^2 = 0.5, 0.7, 0.8, and 0.9, respectively, for the four regions). The means of the differences between the measurements and the model in the four different regions are −3.6, −2.1, 4.8, and 3.6 ppb, respectively. The seasonality of the measurements is also well described by the model in the tropics and in the Southern Hemisphere extratropics. In the Northern Hemisphere extratropics, however, the model methane peaks two to three months earlier than the flask measurements. This is primarily seen at sites northward of 60°N.

[62] Figure A2 shows the same data and model output but binned into five degree latitude bins. The error bars represent one standard deviation of both the variation between sites and the daily variation at one site. The latitudinal gradient described by the flask measurements is reproduced by the model. The model and observed standard deviations are also similar, with a mean standard deviation of 19.4 ppb for the measurements and 14.1 ppb for the model. The latitude range between 20°N and 25°N has a large disagreement, reflecting the increasing divergence seen in Figure A1b.

A2. CARIBIC Aircraft Measurements

[63] The Civil Aircraft for the Regular Investigation of the Atmosphere Based on an Instrument Container (CARIBIC; www.caribic-atmospheric.com) project is a series of atmospheric measurement flights wherein, once a month, an instrument container is installed onboard a commercial long-distance flight beginning in Frankfurt, Germany [*Brenninkmeijer et al.*, 2007; *Schuck et al.*, 2009]. Between 2005 and 2008, 40 flights occurred to eight locations spanning the globe. These measurements allow an evaluation of the model in the free troposphere, typically between 7 and 12 km.

[64] Figure A3a shows the GEOS-Chem model and observed in situ methane number densities from the CARIBIC aircraft flights. The data and model have been averaged over each flight. The error bars represent one standard deviation. The mean difference between the measurements and model is 4.9 ± 9.1 ppb. The variation in the measurements is also well reproduced: the mean of the standard deviation over one flight of the measurements (i.e. the error bars) is 28.9 ppb, while that of the data is 23.9 ppb.

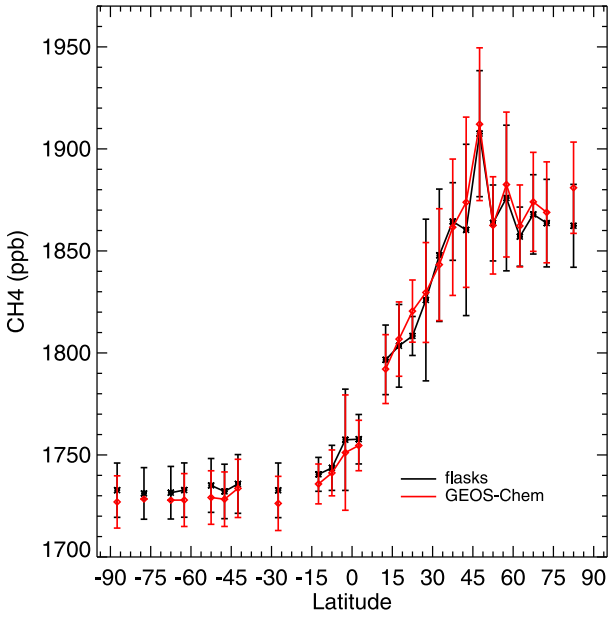

Figure A2. Latitudinal gradient of the flask data and model output, binned over 5 degree latitude bins and averaged over 2005–2008. The error bars represent the standard deviation of the daily values at the site and between sites.

[65] Figure A3b shows the same data and model output but binned into five degree latitude bins. The model reproduces the observed latitudinal gradient, with a mean difference of −0.8 ± 4.1 ppb. The mean of the standard deviation at one latitude of the measurements is 24.0 ppb and 23.3 ppb for the model. In the Southern Hemisphere, the mean difference is −0.1 ± 3.4 ppb. The mean of the standard deviation at one latitude is 16.4 ppb and 15.9 ppb for the measurements and model, respectively.

A3. HALOE

[66] Halogen Occultation Experiment (HALOE) was an infrared filter channel spectrometer on the Upper Atmosphere Research Satellite (UARS), operating between October 1991 and November 2005 [*Russell et al.*, 1993]. Solar occulation was used to measure vertical profiles of several species in the stratosphere, including CH_4. These measurements allow an evaluation of the model in the stratosphere. Figure A4 shows the mean profile retrieved from HALOE and from GEOS-Chem for January to November 2005. Error bars represent one standard deviation. The model has been sampled at the same time and location as the HALOE measurements. Version 19 HALOE CH_4 is used here. Profiles from GEOS-Chem are systematically about 10% larger than the HALOE measurements above 150hPa. The mean difference between the model and the measurements between 0.5 and 185 hPa is −66.3 ppbv, with a standard deviation of 61.5 ppbv. Applying a uniform 10% decrease to the model profile above 150 hPa causes a roughly 10 ppbv change to the calculated XCH_4.

Appendix B: Determining the Position of the Chemical Equator

[67] The Intertropical Convergence Zone (ITCZ) is conventionally defined as the semicontinuous belt of low pressure roughly encircling the equator, located at the ascending branch of the Hadley circulation. The ITCZ effectively forms a transport barrier that inhibits interhemispheric exchange. Previous studies estimate the lifetime associated with hemispheric exchange to be of the order of 1 year [e.g., *Geller et al.*, 1997; *Lintner et al.*, 2004; *Patra et al.*, 2009]. As the distribution of the global methane source is weighted more heavily toward the Northern Hemisphere, a methane concentration gradient exists at the location of the ITCZ. Aircraft carbon monoxide observations from the 2006 ACTIVE campaign taken during pseudo-monsoon conditions observed the interhemispheric chemical gradient above Darwin, between 8.5 and 10°S [*Hamilton et al.*, 2008]. Therefore the chemical equator is not always colocated with the ITCZ.

[68] A GEOS-Chem simulation of an idealized inert tracer was used to determine the position of the chemical gradient. The interhemispheric concentration gradient was constructed by distributing the tracer above the northern side of the convergence zone. Each year analyzed employed a 4 month spin up, that was initialized by defining an initial uniform distribution of tracer north of the 5 °N circle of latitude. Qualitatively, this spin-up time period appeared more than sufficient to allow any initial error in defining the position of the chemical gradient to dissipate before the analysis period. The model's convective parameterization was switched off, as the position of the interhemispheric

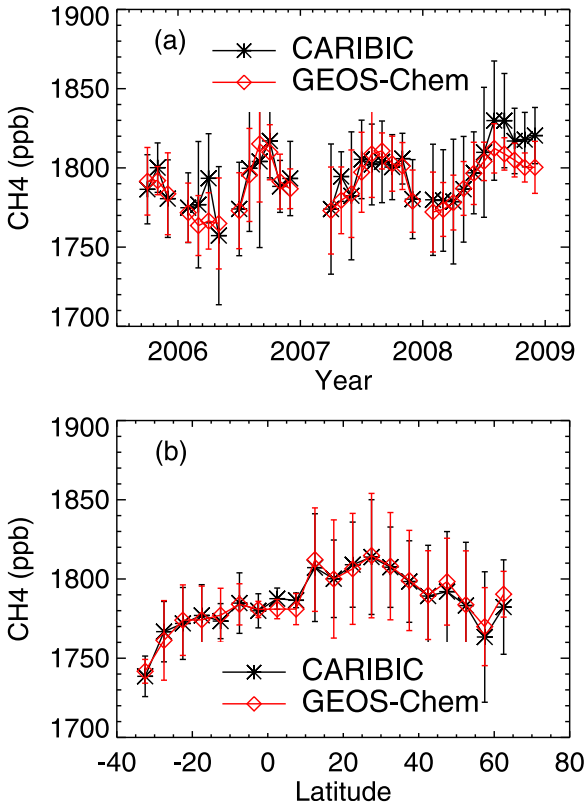

Figure A3. (a) Time series of CARIBIC data and GEOS-Chem model output. Both model and data have been averaged over individual flights. (b) Latitudinal gradient of the data and model output, binned over 5 degree latitude bins. The error bars represent the standard deviation.

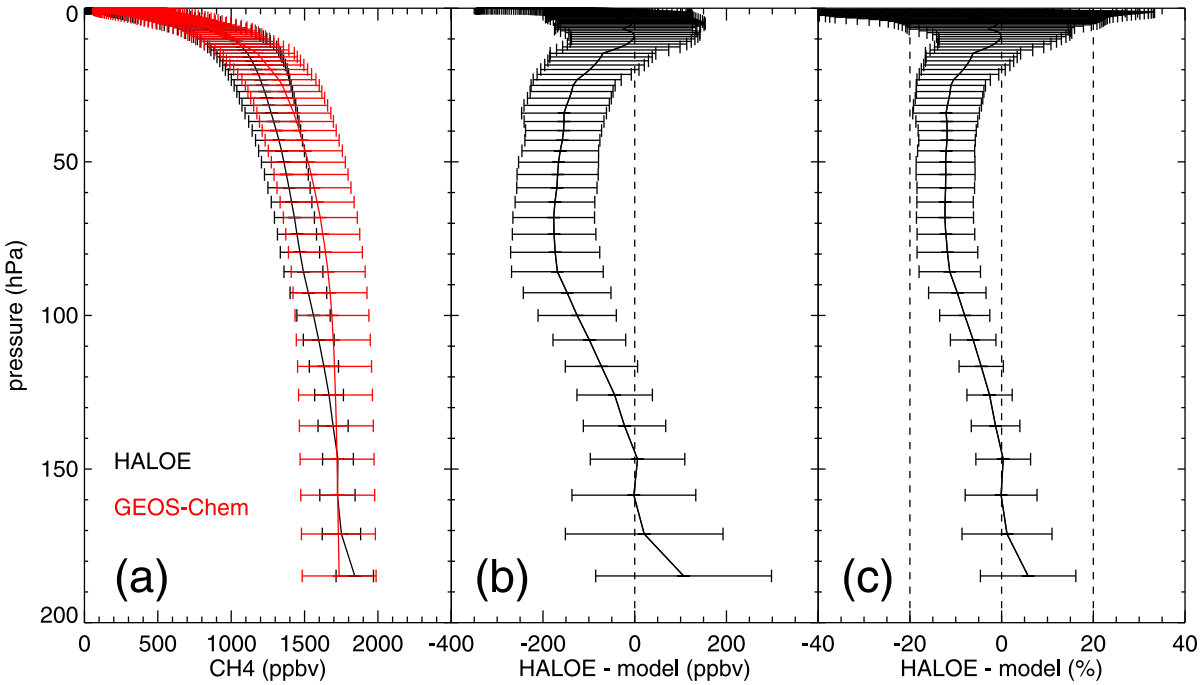

Figure A4. (a) HALOE and model mean profile of methane for 2005. (b) Mean of the absolute difference. (c) Mean of the percentage difference. In all figures the error bars represent the standard deviation of the measurements or model output.

transport barrier forms as a result of patterns in horizontal advective flow.

[69] A simple iterative image processing algorithm was used on each day of the inert tracer simulation, to calculate a threshold value for filtering high tracer concentration gradient values. First, the mean concentration gradient vector magnitude was calculated as an initial guess for the threshold. Grid boxes were separated into two sets, one above and below the threshold guess. A new threshold value was then calculated as the average of the mean values from both sets. This process was repeated until the number of elements of both sets remained unchanged. The southernmost grid boxes above the threshold value were used to identify periods where air being sampled at Darwin belonged to the meteorological northern hemisphere.

[70] **Acknowledgments.** Work at the University of Edinburgh was funded by the UK NERC National Centre for Earth Observation (NCEO). AF's travel to Wollongong was funded by the NCEO and an International Science Linkages grant from the University of Wollongong. Work at the Centre for Atmospheric Chemistry at the University of Wollongong is funded by Australian Research Council projects DP0879468 and LP0562346. TCCON is funded by NASA's terrestrial carbon cycle programme, grant NNX08AI86G. CARIBIC CH_4 data were provided by T. Schuck and C.A.M. Brenninkmeijer. We thank the HALOE science team for the HALOE profiles. The surface measurements were provided by the NASA AGAGE network, the NOAA ESRL network, and the CSIRO Marine and Atmospheric Research GASLab network. We thank three anonymous reviewers for their comments which have helped to improve this manuscript.

References

Bloom, A. A., P. I. Palmer, A. Fraser, D. S. Reay, and C. Frankenberg (2010), Large-scale controls of methanogenesis inferred from methane and gravity spaceborne data, *Science*, *327*(5963), 322–325, doi:10.1126/science.1175176.

Boon, P. I., A. Mitchell, and K. Lee (1997), Effects of wetting and drying on methane emissions from ephemeral floodplain wetlands in south–eastern Australia, *Hydrobiologia*, *357*(1–3), 73–87, doi:10.1023/A:1003126601466.

Brenninkmeijer, C. A. M., et al. (2007), Civil aircraft for the regular investigation of the atmosphere based on an instrumented container: The new CARIBIC system, *Atmos. Chem. Phys.*, *7*, 4953–4976, doi:10.5194/acp-7-4953-2007.

Cunnold, D. M., et al. (2002), In situ measurements of atmospheric methane at GAGE/AGAGE sites during 1985–2000 and resulting source inferences, *J. Geophys. Res.*, *107*(D14), 4225, doi:10.1029/2001JD001226.

Dalal, R. C., D. E. Allen, S. J. Livesley, and G. Richards (2008), Magnitude and biophysical regulators of methane emission and consumption in the Australian agricultural, forest, and submerged landscapes: A review, *Plant Soil*, *309*(1–2), 43–76, doi:10.1007/s11104-007-9446-7.

Department of Climate Change (2010), *Australia's National Greenhouse Accounts – National Inventory Report 2008*, Canberra, Australia. (Available at http://www.climatechange.gov.au/en/climate-change/emissions.aspx.)

Deutscher, N. M., D. W. T. Griffith, C. Paton-Walsh, and R. Borah (2010a), Train-borne measurements of tropical methane enhancements from ephemeral wetlands in Australia, *J. Geophys. Res.*, *115*, D15304, doi:10.1029/2009JD013151.

Deutscher, N. M., et al. (2010b), Total column CO_2 measurements at Darwin, Australia – Site description and calibration against in situ aircraft profiles, *Atmos. Meas. Tech.*, *3*, 947–958, doi:10.5194/amt-3-947-2010.

Dlugokencky, E. J., P. M. Lang, and K. A. Masarie (2009), Atmospheric methane dry air mole fractions from the NOAA ESRL Carbon Cycle Cooperative Global Air Sampling Network, 1983–2008, Version 2011-08-11, Natl. Oceanic and Atmos. Admin., Boulder, Colo. (Available at ftp://ftp.cmdl.noaa.gov/ccg/ch4/flask/event/.)

Fiore, A., D. J. Jacob, H. Liu, R. M. Yantosca, T. D. Fairlie, and Q. Li (2003), Variability in surface ozone background over the United States: Implications for air quality policy, *J. Geophys. Res.*, *108*(D24), 4787, doi:10.1029/2003JD003855.

Francey, R. J., et al. (1996), Global Atmospheric Sampling Laboratory (GASLAB): Supporting and extending the Cape Grim trace gas programs, in *Baseline Atmospheric Program (Australia) 1993*, edited by R.J. Francey, A.L. Dick, and N. Derek, pp. 8–29, Bur. of Meteorol. and CSIRO Div. of Atmos. Res., Melbourne, Victoria, Australia.

Fraser, P. J., R. A. Rasmussen, J. W. Creffield, J. R. French, and M. A. K. Khalil (1986), Termites and global methane - Another assessment, *J. Atmos. Chem.*, *4*(3), 295–310, doi:10.1007/BF00053806.

Fung, I., J. John, J. Lerner, E. Matthews, M. Prather, L. P. Steele, and P. J. Fraser (1991), Three-dimensional model synthesis of the global methane cycle, *J. Geophys. Res.*, *96*(D7), 13,033–13,065, doi:10.1029/91JD01247.

Geller, L. S., J. W. Elkins, J. M. Lobert, A. D. Clarke, D. F. Hurst, J. H. Butler, and R. C. Myers (1997), Tropospheric SF_6: Observed latitudinal distribution and trends, derived emissions and interhemispheric exchange time, *Geophys. Res. Lett.*, *24*(6), 675–678, doi:10.1029/97GL00523.

Griffith, D. W. T. (1996), Synthetic calibration and quantitative analysis of gas phase infrared spectra, *Appl. Spectrosc.*, *50*(1), 59–70.

Griffith, D. W. T. (2002), FTIR measurements of atmospheric trace gases and their fluxes, in *Handbook of Vibrational Spectroscopy*, edited by J. M. Chalmers and P.R. Griffiths, pp. 2823–2841, John Wiley, Hoboken, N. J., doi:10.1002/0470027320.s6802.

Griffith, D., N. Deutscher, P. Krummel, P. Fraser, M.v.d. Schoot, and C. Allison (2011), The UoW FTIR trace gas analyser: Comparison with LoFlo, AGAGE and tank measurements at Cape Grim and GASLAB, in *Baseline Atmospheric Program (Australia) 2007–2008*, edited by P. Krummel and N. Derek, 7–22, CSIRO, Melbourne, Victoria, Australia.

Hamilton, J. F., et al. (2008), Observations of an atmospheric chemical equator and its implications for the tropical warm pool region, *J. Geophys. Res.*, *113*, D20313, doi:10.1029/2008JD009940.

Houweling, S., T. Kaminski, F. Dentener, J. Lelieveld, and M. Heimann (1999), Inverse modeling of methane sources and sinks using the adjoint of a global transport model, *J. Geophys. Res.*, *104*(D21), 26,137–26,160, doi:10.1029/1999JD900428.

Intergovernmental Panel on Climate Change (2007), *Climate Change 2007, The Physical Science Basis. Contribution of Working Group I to the Fourth Assessment Report of the Intergovernmental Panel on Climate Change*, Cambridge Univ. Press, Cambridge, UK.

Karl, D. M., L. Beversdorf, K. M. Björkman, M. J. Church, A. Martinez, and E. F. Delong (2008), Aerobic production of methane in the sea, *Nat. Geosci.*, *1*, 473–478, doi:10.1038/ngeo234.

Kottek, M., J. Grieser, C. Beck, B. Rudolf, and F. Rubel (2006), World Map of the Köppen-Geiger climate classification updated, *Meteorol. Z.*, *15*(3), 259–263.

Lambert, G., and S. Schmidt (1993), Reevaluation of the oceanic flux of methane: Uncertainties and long term variations, *Chemosphere*, *26*(1–4), 579–589, doi:10.1016/0045-6535(93)90443-9.

Lintner, B. R., A. B. Gilliland, and I. Y. Fung (2004), Mechanisms of convection-induced modulation of passive tracer interhemispheric transport interannual variability, *J. Geophys. Res.*, *109*, D13102, doi:10.1029/2003JD004306.

Olivier, J. G. J., J. A. van Aardenne, F. Dentener, L. Ganzeveld, and J. A. H. W. Peters (2005), Recent trends in global greenhouse gas emissions: Regional trends and spatial distribution of key sources, in *Non-CO_2 Greenhouse Gases (NCGG-4)*, edited by A. van Amstel, pp. 325–330, Millpress, Rotterdam.

Patra, P. K., M. Takigawa, G. S. Dutton, K. Uhse, K. Ishijima, B. R. Lintner, K. Miyazaki, and J. W. Elkins (2009), Transport mechanisms for synoptic, seasonal and interannual SF_6 variations and "age" of air in troposphere, *Atmos. Chem. Phys.*, *9*, 1209–1225, doi:10.5194/acp-9-1209-2009.

Prinn, R. G., et al. (2000), A history of chemically and radiatively important gases in air deduced from ALE/GAGE/AGAGE, *J. Geophys. Res.*, *105*(D14), 17,751–17,792, doi:10.1029/2000JD900141.

Prinn, R. G., et al. (2005), Evidence for variability of atmospheric hydroxyl radicals over the past quarter century, *Geophys. Res. Lett.*, *32*, L07809, doi:10.1029/2004GL022228.

Rigby, M., et al. (2008), Renewed growth of atmospheric methane, *Geophys. Res. Lett.*, *35*, L22805, doi:10.1029/2008GL036037.

Roshier, D. A., and R. M. Rumbachs (2004), Broad-scale mapping of temporary wetlands in arid Australia, *J. Arid Environ.*, *56*(2), 249–263, doi:10.1016/S0140-1963(03)00051-X.

Roshier, D. A., P. H. Whetton, R. J. Allan, and A. I. Robertson (2001), Distribution and persistence of temporary wetland habitats in arid Australia in relation to climate, *Austral. Ecol.*, *26*(4), 371–384, doi:10.1046/j.1442-9993.2001.01122.x.

Russell, J. M., III, L. L. Gordley, J. H. Park, S. R. Drayson, W. D. Hesketh, R. J. Cicerone, A. F. Tuck, J. E. Frederick, J. E. Harries, and P. J. Crutzen (1993), The Halogen Occultation Experiment, *J. Geophys. Res.*, *98*(D6), 10,777–10,797, doi:10.1029/93JD00799.

Schuck, T. J., C. A. M. Brenninkmeiher, F. Slemr, I. Xueref-Remy, and A. Zahn (2009), Greenhouse gas analysis of air samples collected onboard the CARIBIC passenger aircraft, *Atmos. Meas. Tech.*, *2*, 449–464, doi:10.5194/amt-2-229-2009.

Tapley, B. D., S. Bettadpur, J. C. Ries, P. F. Thompson, and M. M. Watkins (2004), GRACE measurements of mass variability in the Earth system, *Science*, *305*(5683), 503–505, doi:10.1126/science.1099192.

van der Werf, G. R., J. T. Randerson, L. Giglio, G. J. Collatz, P. S. Kasibhatla, and A. F. Arellano Jr. (2006), Interannual variability in global biomass burning emissions from 1997 to 2004, *Atmos. Chem. Phys.*, *6*, 3423–3441, doi:10.5194/acp-6-3423-2006.

Wang, Y.-P., and S. T. Bentley (2002), Development of a spatially explicit inventory of methane emissions from Australia and its verification using atmospheric concentration data, *Atmos. Environ.*, *36*(31), 4965–4975, doi:10.1016/S1352-2310(02)00589-7.

Wang, J. S., J. A. Logan, M. B. McElroy, B. N. Duncan, I. A. Megretskaia, and R. M. Yantosca (2004), A 3-D model analysis of the slowdown and interannual variability in the methane growth rate from 1988 to 1997, *Global Biogeochem. Cycles*, *18*, GB3011, doi:10.1029/2003GB002180.

Wheeler, M. C., and J. L. McBride (2005), Australian-Indonesian monsoon, in *Intraseasonal Variability in the Atmosphere-Ocean System*, edited by W. K.M. Lau and D. E. Waliser, pp. 125–173, Springer, Berlin, doi:10.1007/3-540-27250-X5.

Wunch, D., et al. (2010), Calibration of the total carbon column observing network using aircraft profile data, *Atmos. Meas. Tech.*, *3*, 1351–1362, doi:10.5194/amt-3-1351-2010.

Wunch, D., G. C. Toon, J.-F.L. Blavier, R. Washenfelder, J. Notholt, B. J. Connor, D. W. T. Griffith, V. Sherlock, and P. O. Wennberg (2011), The Total Carbon Column Observing Network (TCCON), *Philos. Trans. R. Soc. London, Ser. A*, *369*(1943), 2087–2112, doi:10.1098/rsta.2020.0240.

Yevich, R., and J. A. Logan (2003), An assessment of biofuel use and burning of agricultural waste in the developing world, *Global Biogeochem. Cycles*, *17*(4), 1095, doi:10.1029/2002GB001952.

C. Chan Miller, Department of Earth and Planetary Sciences, Harvard University, Cambridge, MA 02138, USA.

N. M. Deutscher, Institute of Environmental Physics, University of Bremen, D-28359 Bremen, Germany.

A. Fraser and P. I. Palmer, School of GeoSciences, University of Edinburgh, Edinburgh, EH9 3JN, UK. (ac.fraser@ed.ac.uk)

D. W. T. Griffith and N. B. Jones, School of Chemistry, University of Wollongong, Wollongong, NSW 2522, Australia.